Peptidylarginine deiminase 4 promotes age-related organ fibrosis

Kimberly Martinod,[1,3]* Thilo Witsch,[1,3]* Luise Erpenbeck,[1,3]* Alexander Savchenko,[1,3] Hideki Hayashi,[1,3] Deya Cherpokova,[1,3] Maureen Gallant,[1] Maximilian Mauler,[4,5] Stephen M. Cifuni,[1] and Denisa D. Wagner[1,2,3]

[1]Program in Cellular and Molecular Medicine and [2]Division of Hematology/Oncology, Boston Children's Hospital, Boston, MA 02115
[3]Department of Pediatrics, Harvard Medical School, Boston, MA 02115
[4]Faculty of Biology and [5]Department of Cardiology and Angiology I, Heart Center, University of Freiburg, 79106 Freiburg, Germany

Aging promotes inflammation, a process contributing to fibrosis and decline in organ function. The release of neutrophil extracellular traps (NETs [NETosis]), orchestrated by peptidylarginine deiminase 4 (PAD4), damages organs in acute inflammatory models. We determined that NETosis is more prevalent in aged mice and investigated the role of PAD4/NETs in age-related organ fibrosis. Reduction in fibrosis was seen in the hearts and lungs of aged PAD4$^{-/-}$ mice compared with wild-type (WT) mice. An increase in left ventricular interstitial collagen deposition and a decline in systolic and diastolic function were present only in WT mice, and not in PAD4$^{-/-}$ mice. In an experimental model of cardiac fibrosis, cardiac pressure overload induced NETosis and significant platelet recruitment in WT but not PAD4$^{-/-}$ myocardium. DNase 1 was given to assess the effects of extracellular chromatin. PAD4 deficiency or DNase 1 similarly protected hearts from fibrosis. We propose a role for NETs in cardiac fibrosis and conclude that PAD4 regulates age-related organ fibrosis and dysfunction.

INTRODUCTION

In both humans and mice, organ function deteriorates during aging (Biernacka and Frangogiannis, 2011; Wynn and Ramalingam, 2012). This is at least in part caused by fibrosis, an excessive deposition of extracellular matrix (ECM) components such as collagen (Wynn and Ramalingam, 2012). In this process, functional parenchymal organ tissue is replaced by fibrotic tissue, which can severely diminish organ function. Fibrosis typically results from chronic inflammation induced by a variety of stimuli, including persistent immune reactions, radiation, and chemical or mechanical tissue injury (Wynn and Ramalingam, 2012). In spite of the well-known connection between fibrosis and inflammation, the role of neutrophilic granulocytes in fibrosis in general and in age-related organ fibrosis in particular remains elusive. In response to activating signals, neutrophils produce reactive oxygen species (ROS; Clark, 1999), which have been shown to regulate collagen synthesis in cardiac fibroblasts (Siwik et al., 2001; Sirker et al., 2007), providing a possible link between cardiac fibrosis and neutrophils. Furthermore, ROS generation in neutrophils increases with age in humans (Ogawa et al., 2008). ROS also induce neutrophil extracellular trap (NET) formation (NETosis), a recently described antimicrobial defense mechanism of neutrophils. Here, activated neutrophils release their chromatin as NETs covered with antimicrobial peptides to trap and kill pathogens (Brinkmann et al., 2004). This process depends on the enzyme peptidylarginine deiminase 4 (PAD4), which citrullinates specific arginine residues on histone tails, resulting in the chromatin decondensation necessary for the release of NETs (Wang et al., 2009). NETosis also occurs under noninfectious conditions such as hypoxia (De Meyer et al., 2012), inflammation, and autoimmune diseases (Kolaczkowska and Kubes, 2013). NETs are injurious to underlying tissue and are proinflammatory and prothrombotic (Fuchs et al., 2012; Demers and Wagner, 2013; Martinod and Wagner, 2014). Using PAD4$^{-/-}$ mice or recombinant human DNase (rhDNase) 1 infusion (which cleaves NETs) in WT mice, our group has previously shown that extracellular DNA/NETs have deleterious effects on heart function in the setting of acute myocardial injury (Savchenko et al., 2014a), providing additional evidence for the proinflammatory role of NETs. NET release is triggered under many pathological conditions, such as deep vein thrombosis (Fuchs et al., 2010; Brill et al., 2012; Martinod et al., 2013), transfusion-related acute lung injury (Caudrillier et al., 2012; Thomas et al., 2012), myocardial ischemia/reperfusion (Savchenko et

*K. Martinod, T. Witsch, and L. Erpenbeck contributed equally to this paper.

Correspondence to Denisa D. Wagner: denisa.wagner@childrens.harvard.edu

T. Witsch's present address is Dept. of Cardiology and Angiology I, Heart Center, University of Freiburg, 79106 Freiburg, Germany.

L. Erpenbeck's present address is Dept. of Dermatology, Venereology, and Allergology, University Medical Center Göttingen, 37075 Göttingen, Germany.

Abbreviations used: AAC, ascending aortic constriction; ECM, extracellular matrix; H3Cit, citrullinated histone H3; IVS, interventricular septum; LVEF, left ventricular ejection fraction; LVID, left ventricular inner diameter; LVPW, left ventricular posterior wall; NET, neutrophil extracellular traps; rhDNase, recombinant human DNase; ROS, reactive oxygen species.

© 2017 Martinod et al. This article is distributed under the terms of an Attribution–Noncommercial–Share Alike–No Mirror Sites license for the first six months after the publication date (see http://www.rupress.org/terms/). After six months it is available under a Creative Commons License (Attribution–Noncommercial–Share Alike 4.0 International license, as described at https://creativecommons.org/licenses/by-nc-sa/4.0/).

The Rockefeller University Press $30.00
J. Exp. Med. 2017 Vol. 214 No. 2 439–458
https://doi.org/10.1084/jem.20160530

The Journal of Experimental Medicine

Downloaded from http://rupress.org/jem/article-pdf/214/2/439/1756691/jem_20160530.pdf by guest on 08 February 2026

al., 2014a), atherosclerosis (Borissoff et al., 2013; Quillard et al., 2015; Warnatsch et al., 2015), autoimmune diseases (Radic and Marion, 2013), and cancer (Demers et al., 2012; Cools-Lartigue et al., 2013), where they significantly contribute to disease progression. Recently, fibroblasts were shown to undergo transdifferentiation to collagen-depositing myofibroblasts after incubation with NETs in vitro, and NETs were identified in proximity to α-smooth muscle actin–positive fibroblasts in tissue sections from patients with fibrotic interstitial lung disease (Chrysanthopoulou et al., 2014).

Both fibrosis and inflammation are closely associated with aging (Varagic et al., 2001). It is known that elderly persons experience significant changes in the function of their immune system, including a decline in the adaptive immune system, which creates an imbalance between adaptive and innate immune responses (Aw et al., 2007). Generally, aging leads to a more proinflammatory environment (Meyer et al., 1998), with higher numbers of neutrophils (Sohal and Weindruch, 1996; Ogawa et al., 2008) along with an increased susceptibility to pathogens and a higher incidence of inflammatory diseases (Aw et al., 2007), such as neurodegenerative disorders, rheumatoid arthritis, osteoporosis, diabetes, cardiovascular disease, and thrombosis (Tabas and Glass, 2013). Intriguingly, many of these illnesses have been reported to involve NETs (Azevedo et al., 2012; Savchenko et al., 2014a; Sur Chowdhury et al., 2014; Wong et al., 2015; Zenaro et al., 2015). Whether NETosis may be more prominent in aging has not been rigorously evaluated.

Both the heart and the lung appear to be susceptible to age-related fibrosis in humans and mice. Fibrotic lung diseases are characterized by enhanced collagen deposition in the airways, including the alveolar walls, and subsequent disturbance of pulmonary gas exchange. Excessive fibrotic tissue remodeling is a predominant feature of many chronic lung diseases affecting mainly the older population (van Durme et al., 2009; Afonso et al., 2011; Navaratnam et al., 2011). In cardiac aging, fibrotic remodeling may lead to diastolic dysfunction caused by increased ventricular stiffness and, possibly, systolic heart failure (Wei, 1992), which is the most common cause of hospitalization in patients older than 65 yr (DeFrances et al., 2007). Pressure overload to the left ventricle caused by arterial hypertension or aortic valve stenosis is very common in the elderly population. Over time, the increase in afterload leads to myocardial hypertrophy, cardiac fibrosis, ventricular stiffening, and subsequent congestive heart failure (Lorell and Carabello, 2000), which bears substantial morbidity and mortality. There is evidence that the fibrotic changes in afterload-stressed hearts may, at least in part, result from up-regulation of proinflammatory cytokines in the cardiac tissue (Sun et al., 2007). Given the need for a better understanding of the complex mechanisms linking inflammation to fibrosis and aging, the goal of this study was to address the putative interplay between PAD4, NET release, aging, and organ fibrosis.

RESULTS

Neutrophil susceptibility to form NETs increases with mouse age

There are many changes that occur in the aging immune system, including an increase in hematopoietic stem cells of the myeloid lineage versus cells of the lymphoid lineage (Beerman et al., 2010). To further study the effect of aging in mice, we examined blood and neutrophils from young (8–16 wk) and old (20–27 mo) mice obtained from the National Institutes of Health's C57BL/6NIA Aged Rodent Colony. We were able to confirm that in these mice, neutrophil counts were elevated with age (Fig. 1 A), along with platelet counts (Fig. 1 B). More platelet–neutrophil complexes were seen in older mice than in younger mice, indicating a greater extent of platelet activation and platelet–neutrophil interaction (Fig. 1 C). We also saw that a higher percentage of circulating leukocytes were neutrophils in the old mice by immunostaining cytospin preparations of peripheral blood leukocytes for the neutrophil-specific marker Ly6G (Fig. 1 D). Using citrullinated histone H3 (H3Cit) as a biomarker of PAD4 activity and neutrophil priming for NETosis, we examined basal levels of circulating $H3Cit^+$ cells and found that a greater percentage of neutrophils were primed toward NETosis in the old mice (Fig. 1 E). To evaluate whether neutrophils from the older animals had a greater tendency to release NETs, we isolated peripheral blood neutrophils and stimulated them with calcium ionophore or PMA. We found that after incubation, either with or without stimulation, neutrophils from older mice had a greater propensity to form NETs as quantified by microscopy (Fig. 1 F).

We then investigated $PAD4^{-/-}$ and WT mice housed in our animal facility on a C57BL/6J background. Neutrophil count was similarly elevated in older (14–17 mo old) WT or $PAD4^{-/-}$ mice compared with younger (6–14 wk old) mice (Fig. 2 A). Platelet counts were also elevated with age in both genotypes (Fig. 2 B). These elevations were less dramatic than those seen in 20–24-mo-old mice in Fig. 1 (A and B), likely because of their younger age. Neutrophil percentage did not change with age (Fig. 2 C); however, more circulating $H3Cit^+$ neutrophils were found in old WT mice (Fig. 2 D). Not surprisingly, the percentage of neutrophils forming NETs after incubation in vitro was also elevated in old WT C57BL/6J mice (Fig. 2 E). Next, we examined platelet–neutrophil complexes in peripheral blood from these mice and saw an age-related increase in both WT and $PAD4^{-/-}$ mice. However, there were significantly fewer platelet–neutrophil complexes in old $PAD4^{-/-}$ compared with old WT mice (Fig. 2 F). As activated platelets are a physiological trigger of NET formation via the P-selectin–PSGL-1 interaction (Etulain et al., 2015), which mediates platelet–neutrophil complex formation, this may contribute to spontaneous NET formation in older animals. Platelets are also a main source of plasma TGFβ, which drives fibrosis (Meyer et al., 2012). TGFβ is stored in α-granules in platelets, and upon activation, released TGFβ can be detected on platelets by flow cytometry. We induced platelet

Downloaded from http://rupress.org/jem/article-pdf/214/2/439/1756691/jem_20160530.pdf by guest on 08 February 2026

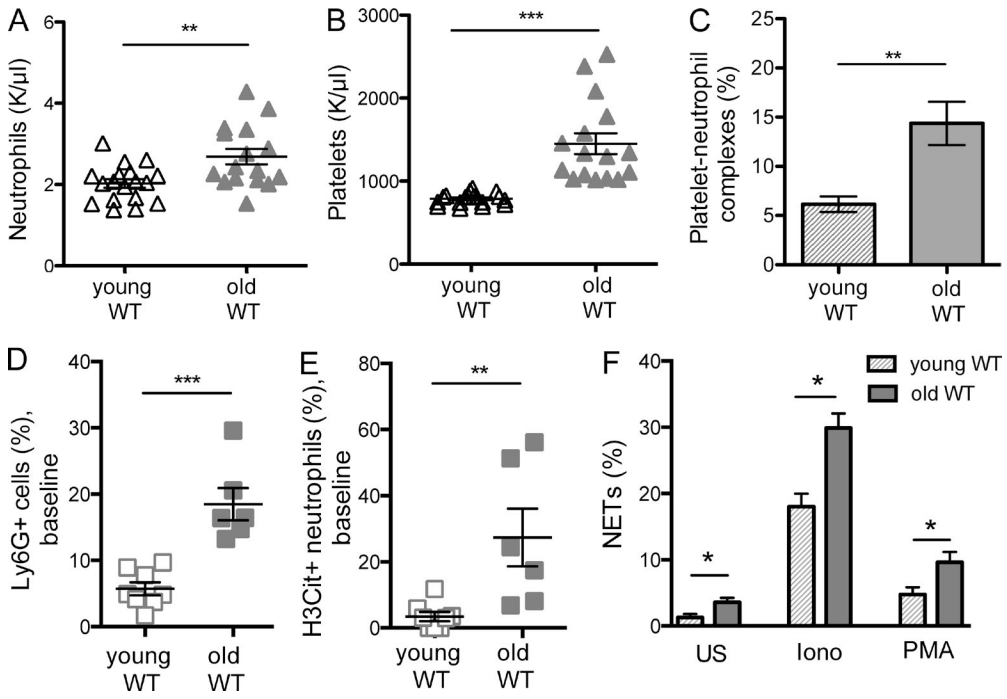

Figure 1. **Increased neutrophil and platelet count, formation of platelet–neutrophil complexes, and neutrophil susceptibility to produce NETs in aged C57BL/6NIA mice.** (A) Neutrophil counts in peripheral blood of young (2 mo) versus old (20–24 mo) WT mice; $n = 16–18$. (B) Platelet counts in young (2 mo) versus old (20–24 mo) WT mice; $n = 16–18$. (C) Quantification by flow cytometry of platelet–neutrophil complexes ($CD41^+Ly6G^+$) in whole blood collected from young (2–3 mo) and old (20–24 mo) mice; $n = 7–12$. (D) Quantification of Ly6G-positive neutrophils in cytospins of the total leukocyte population; $n = 6–8$. (E) Quantification of the percentage of H3Cit-positive neutrophils by thresholding analysis of immunostained cytospins of RBC-depleted blood cells; $n = 6–8$. In D and E, young mice were 6–8 wk old and old mice were 15–20 mo old. (F) Percentage of NET-forming peripheral blood neutrophils after incubation with vehicle (unstimulated [US]), 4 µM ionomycin (Iono), or 100 nM PMA for 3.5 h. Neutrophils from old (24–27 mo) mice formed significantly more NETs under all conditions than neutrophils from young (2–5 mo) mice; $n = 5$. *, $P < 0.05$; **, $P < 0.01$; ***, $P < 0.001$ by Student's *t* test. The graphs show mean and SEM from 16–18 (A and B), 7–12 (C), 6–8 (D and E), and 5 (F) mice per group from five (A and B), three (C), or two (D–F) independent experiments.

degranulation with a combination of ADP and U46619 (a thromboxane A2 stable analogue) and quantified the percentage of platelets highly positive for TGFβ (Fig. 2 G). Old WT but not old $PAD4^{-/-}$ mice had a significant increase in percent of TGFβ-positive platelets compared with cells from young mice of either genotype (Fig. 2 G). There is likely increased crosstalk between platelets and neutrophils with aging that promotes neutrophil activation and other negative consequences associated with increased formation of platelet–leukocyte complexes (Wagner and Frenette, 2008).

These observations indicate that in aging WT mice, NET formation is likely to be exacerbated by both increased neutrophil counts and increased neutrophil priming. We hypothesized that increased propensity to NETosis, and the deleterious effects of NET formation, may over time lead to organ fibrosis and dysfunction and that the organs of animals not producing NETs would fare better as they aged.

$PAD4^{-/-}$ mice are protected from age-related decline in heart function

We compared the lung and heart aging process of WT to $PAD4^{-/-}$ mice that do not make NETs. We performed functional analyses on WT and $PAD4^{-/-}$ retired breeders (12–17 mo old) using age- and sex-matched groups of males and females. The mice were housed in the same animal room and had received an enriched "reproduction diet" throughout their life. Both genotypes of mice had normal blood oxygen saturation (SpO_2: WT, 98.5% ± 0.46, $n = 6$; $PAD4^{-/-}$, 98.2% ± 0.21, $n = 9$; $P = 0.46$). This was expected, as blood oxygenation declines only in the setting of severe heart or lung failure in mice. We then used echocardiography to measure structural and functional parameters of the heart in both genotypes (Fig. 3 A). We evaluated the left ventricular ejection fraction (LVEF) and found that WT retired breeders showed a decline in their LVEF to 50.7% (Fig. 3 B), consistent with literature on heart function in aging WT mice (Yang et al., 1999). Surprisingly, however, old $PAD4^{-/-}$ retired breeders had a significantly better heart function, with a mean LVEF of 61.2%, comparable with the LVEF of young mice (Fig. 3 B, first panel). End-diastolic dimensions of the heart such as the diameter of the interventricular septum (IVS;d), the left ventricular posterior wall (LVPW;d), and left ventricular inner diameter (LVID;d) were assessed in both groups of mice (Fig. 3 B) to check for possible significant dimensional differences such as severe ventricular dilation or wall

Downloaded from http://rupress.org/jem/article-pdf/214/2/439/1756691/jem_20160530.pdf by guest on 08 February 2026

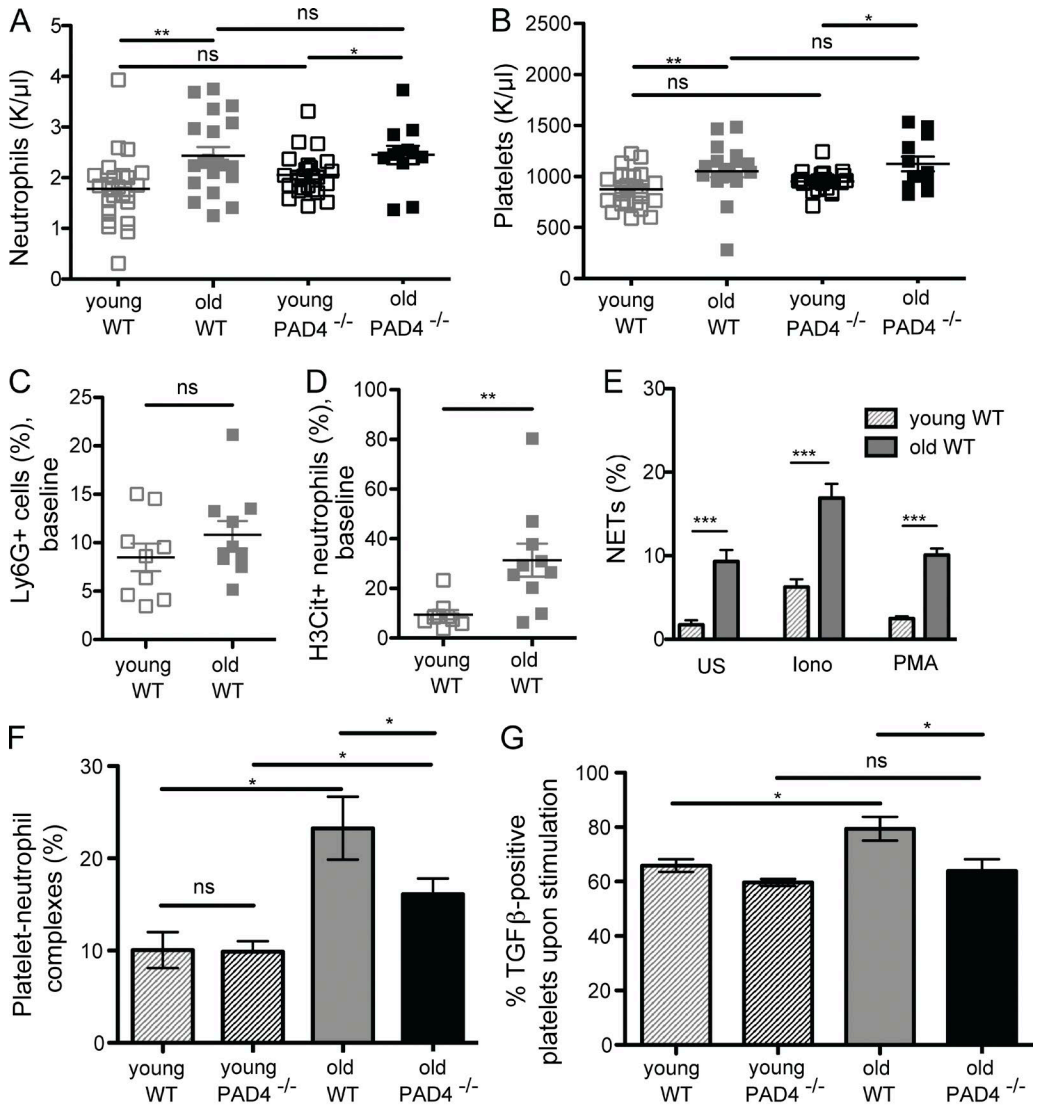

Figure 2. **Neutrophils and platelets in aging WT or PAD4$^{-/-}$ C57BL/6J mice.** (A and B) Neutrophil (A) and platelet (B) counts in peripheral blood of young (2 mo) versus aging (14–17 mo) WT or PAD4$^{-/-}$ mice; n = 12–24. (C) Quantification of Ly6G-positive neutrophils in the total leukocyte population; n = 9–10. (D) Quantification of the percentage of H3Cit-positive neutrophils by thresholding analysis; n = 9–10. (E) Percentage of NET-forming isolated peripheral blood neutrophils after 3.5 h of ex vivo incubation with vehicle (US), 4 µM ionomycin (Iono), or 200 nM PMA for 3.5 h; n = 8. (F) Quantification by flow cytometry of platelet–neutrophil complexes (CD41^{+}Ly6G^{+}) in whole blood; n = 7–12. (G) TGFβ expression on activated platelets was determined by flow cytometric analysis in diluted whole blood stimulated with 10 µM ADP + 3 µM U46619; n = 6–11. Significance was determined by Student's t test. *, P < 0.05; **, P < 0.01; ***, P < 0.001. The graphs show mean and SEM from 12–24 (A and B), 9–10 (C and D), 8 (E), 7–12 (F), or 6–11 (G) mice per group from four (A, B, and F), three (G), or two (C–E) independent experiments.

hypertrophy that could underlie the observed changes in heart function. None of the measured structural parameters yielded significant differences between the two genotypes, suggesting that myocardial contractility and thus heart function itself are compromised in old WT but not PAD4$^{-/-}$ breeders. Of note, blood pressure was not significantly different between the two aged genotypes (WT: 93.38 ± 1.59, n = 9; PAD4$^{-/-}$: 95.48 ± 2.95 mm Hg, n = 10; P = 0.65).

To eliminate the possible metabolic effects of the reproduction diet received by the retired breeders, we repeated all measurements with 14–18-mo-old WT and PAD4$^{-/-}$ mice that were allowed to age on standard laboratory diet. Young, gender-matched mice were 6–8 wk old and housed in the same animal room. Again, the old WT mice showed a decline in LVEF (Fig. 3 C) compared with the young WT mice, with LVEF values similar to those observed in the retired WT breeders. This indicates that the reduction in heart function in old mice was independent of the dietary factors in our study. In this second group, the old PAD4$^{-/-}$ mice again had a significantly higher mean LVEF that was com-

Downloaded from http://rupress.org/jem/article-pdf/214/2/439/1756691/jem_20160530.pdf by guest on 08 February 2026

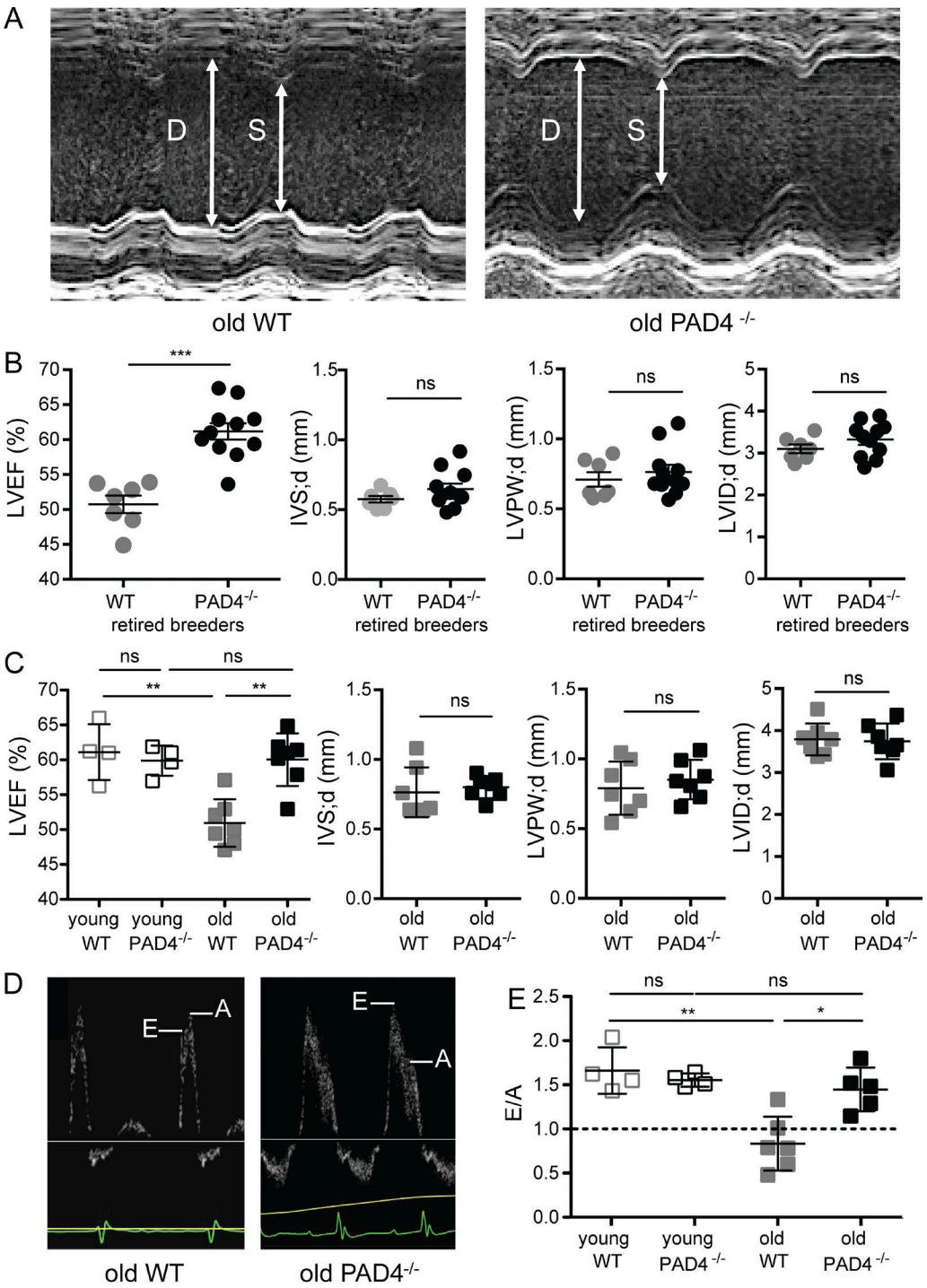

Figure 3. **PAD4$^{-/-}$ mice are protected from age-related decline in systolic and diastolic heart function compared with WT mice.** (A and B) LVEF, as a measure of systolic function, and cardiac dimensions (IVS;d, LVPW;d, and LVID;d) of WT and PAD4$^{-/-}$ retired breeders (12–17 mo) were measured by transthoracic echocardiography. (A) Representative ultrasound M-mode images of the left ventricle in an old PAD4$^{-/-}$ mouse compared with an old WT mouse. D, diastole; S, systole. (B) Quantification of LVEF (left) and cardiac dimensions (right panels) in WT and PAD4$^{-/-}$ retired breeders; n = 7–11. (C) The same echocardiographic measurements of LVEF (left) and cardiac dimensions (right) were repeated in a group of young (6–8 wk) and old (14–18 mo) WT and PAD4$^{-/-}$ mice that had been kept on standard laboratory diet; n = 4–7. (D and E) Ventricular diastolic dysfunction was evaluated in young WT and PAD4$^{-/-}$ (6–8 wk) mice as well as old WT and PAD4$^{-/-}$ mice (15–20 mo). The flow pattern across the mitral valve was assessed using pulsed wave Doppler mode, and the ventricular filling pattern was calculated as the ratio between the E and A wave. (D) Characteristic images of pulsed wave Doppler measurements of the E and A wave showed a normal E/A pattern (E > A) in the old PAD4$^{-/-}$ mice and a reversed pattern (E < A) in the old WT mice (A was taller than

Downloaded from http://rupress.org/jem/article-pdf/214/2/439/1756691/jem_20160530.pdf by guest on 08 February 2026

parable to the means seen in young PAD4$^{-/-}$ or WT mice (Fig. 3 C, first panel). This corroborates that PAD4$^{-/-}$ mice are protected from an age-dependent decline in heart function. Measurement of structural parameters again showed similar heart dimensions for old WT and PAD4$^{-/-}$ mice on standard diet, with no significant differences for IVS;d, LVPW;d, and LVID;d (Fig. 3 C).

In contrast to the notable decline in LVEF seen in mice with old age, in humans, age-associated decline of heart function is mostly associated with diastolic dysfunction (Pugh and Wei, 2001; Loffredo et al., 2014). For that reason, we evaluated signs of diastolic dysfunction in a set of old WT (14–20 mo) and old PAD4$^{-/-}$ (18 mo) mice on standard diet and compared with young WT and PAD4$^{-/-}$ (2 mo) mice. Specifically, the diastolic mitral inflow pattern was measured by echocardiography (Fig. 3, D and E), and the ratio between the E-wave (representing the early, passive filling of the ventricle) and the A-wave (representing the active filling of the ventricle by the atrial contraction) was calculated. Generally, an E/A ratio of less than 1 is considered a sign of impaired ventricular relaxation and, hence, diastolic dysfunction, which can be caused by increased stiffness of the heart. In the old WT nonbreeder mice, the mean E/A ratio was 0.83, corroborating our previous observation of heart dysfunction in these mice (Fig. 3, D [left] and E). In contrast, none of the PAD4$^{-/-}$ old nonbreeders showed signs of diastolic dysfunction; the mean E/A ratio was 1.44 and significantly higher compared with old WT mice (Fig. 3, D [right] and E). Unlike the old WT mice, old PAD4$^{-/-}$ mice did not have a significant decline in E/A ratio compared with young PAD4$^{-/-}$ mice. Thus, in the PAD4$^{-/-}$ mice, healthy heart function was preserved in old age.

PAD4$^{-/-}$ mice have significantly less interstitial myocardial fibrosis than age-matched WT mice

Collagen content increases with age in human hearts (Gazoti Debessa et al., 2001). Age-related structural remodeling of the human heart and decline of heart function is associated with cardiomyocyte hypertrophy and interstitial fibrosis. In young, healthy hearts, myocytes and myocardial bundles are surrounded by thin layers of connective tissue: the endomysium and perimysium, respectively. In contrast, with age, ECM proteins accumulate in the interstitium and result in endomysial and perimysial fibrosis (Biernacka and Frangogiannis, 2011). We therefore assessed cardiac fibrosis for both WT and PAD4$^{-/-}$ genotypes in the retired breeders and also in the old nonbreeders and young mice.

We harvested the hearts of WT and PAD4$^{-/-}$ retired breeders (n = 6) and assessed interstitial heart fibrosis by Sirius red stain, which is used to identify and quantify collagen in cardiac tissue (Fig. 4, A–D; Junqueira et al., 1979; Namba et al., 1997; Ammarguellat et al., 2001). We used this microscopy-based approach so that perivascular staining could be distinguished and excluded from this analysis. Interestingly, WT retired breeders showed significantly more interstitial fibrosis than the age-matched (12–17 mo) PAD4$^{-/-}$ breeders (Fig. 4, A and D). In contrast to WT, collagen fibers in the PAD4$^{-/-}$ breeder hearts were mainly located in proximity to vessels, with only a scattered pattern of focal interstitial fibrosis (Fig. 4 D, right). We performed the same analysis in the old WT and PAD4$^{-/-}$ nonbreeders and found a similar difference between the WT and PAD4$^{-/-}$ mice (Fig. 4 B). Additionally, the hearts of young WT and PAD4$^{-/-}$ mice were assessed to determine whether a fibrosis difference between the genotypes was already present at an early age. At 6–8 wk, WT and PAD4$^{-/-}$ mice had comparably low interstitial heart fibrosis (Fig. 4, B and C). Therefore, the observed difference between WT and PAD4$^{-/-}$ mice was indeed an age-related phenomenon. Remarkably, in the old PAD4$^{-/-}$ nonbreeders, the amount of fibrotic tissue remained similar to that of young PAD4$^{-/-}$ or WT mice (Fig. 4 B), indicating that those old mice were protected from age-related myocardial interstitial fibrosis. Increased fibrosis in old WT compared with old PAD4$^{-/-}$ myocardium could also be observed qualitatively by Masson's trichrome staining (Fig. 4 D, right), another type of staining commonly used to visualize collagen and fibrotic tissue changes (Bancroft and Gamble, 2008; Savchenko et al., 2014b). We immunostained cryosections of hearts from old WT and PAD4$^{-/-}$ mice with an antibody specific for type I collagen to confirm that these interstitial fibers indeed contained collagen (Fig. 4 E).

To address whether the observed difference in fibrosis between old WT and old PAD4$^{-/-}$ mice was associated with the difference of heart function between the two genotypes, we correlated myocardial fibrosis and LVEF of all mice. Indeed, the correlation analysis showed a significant ($P < 0.02$) negative correlation, with a Pearson correlation coefficient (r) of −0.42 (Fig. 4 F). Although this result does not exclude additional factors in the development of heart dysfunction, it is thought that fibrosis determines tissue properties such as stiffness (Wei, 1992; Biernacka and Frangogiannis, 2011) and thus cardiac function in these mice.

Age-related interstitial pulmonary fibrosis is reduced in PAD4$^{-/-}$ mice compared with WT mice

The lung is an organ highly susceptible to fibrosis (van Durme et al., 2009; Navaratnam et al., 2011). We performed histological analyses on WT and PAD4$^{-/-}$ retired breeders. The lungs of retired PAD4$^{-/-}$ breeders showed significantly less interstitial fibrosis compared with WT retired breeders, as

E), leading to a ratio of <1. (E) Quantification of the E/A ratio in young and old WT and PAD4$^{-/-}$ mice. An E/A ratio <1 is evidence of impaired ventricular relaxation; n = 4–6. *, $P < 0.05$; **, $P < 0.01$; ***, $P < 0.001$ by Mann–Whitney U test. The graphs show mean and SEM from 7–11 (A and B), 4–7 (C), and 4–6 (D and E) mice per group from four (A and B) or two (C–E) independent experiments.

Downloaded from http://rupress.org/jem/article-pdf/214/2/439/1756691/jem_20160530.pdf by guest on 08 February 2026

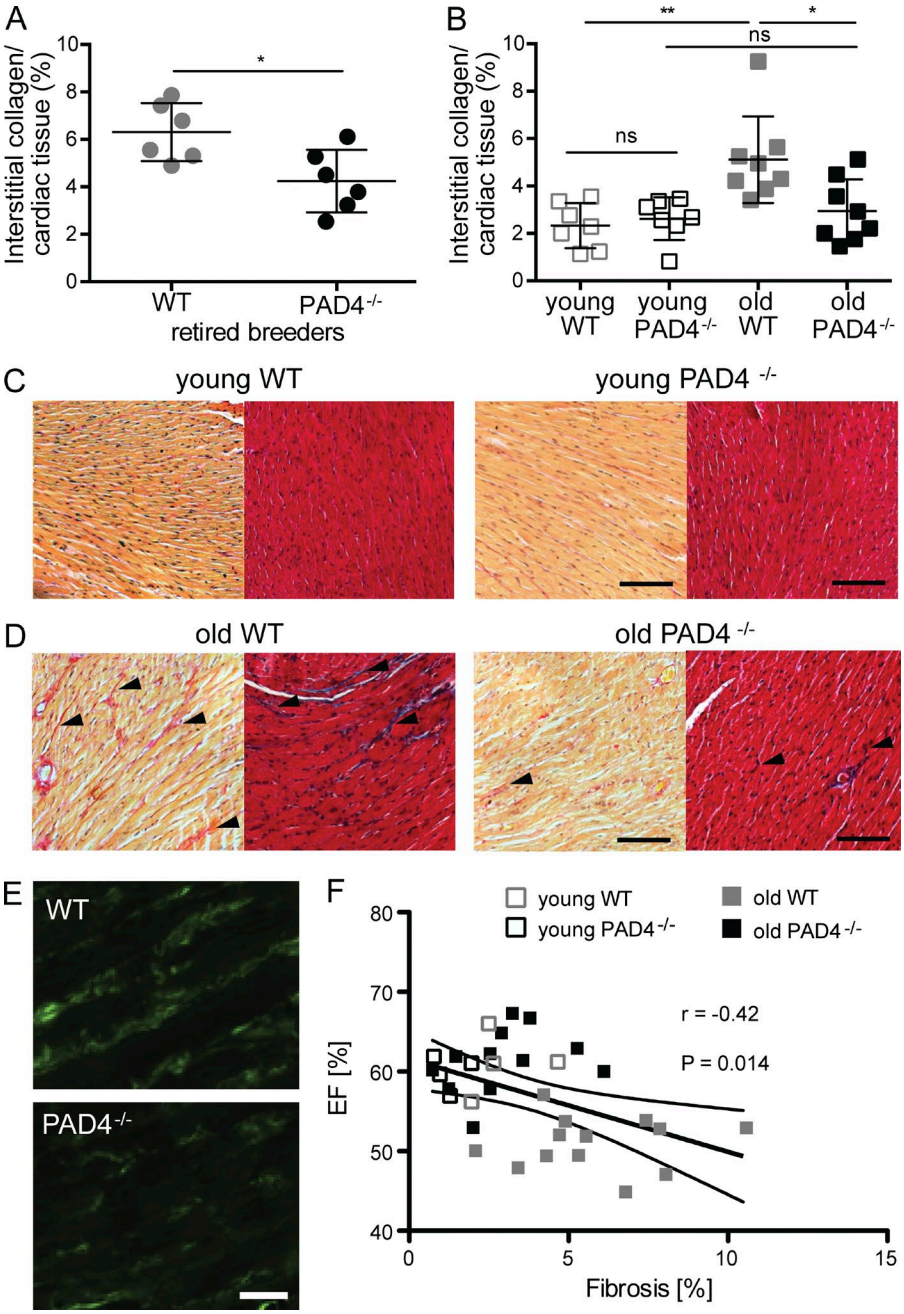

Figure 4. **PAD4 deficiency reduces age-related cardiac fibrosis.** (A) Cardiac interstitial fibrosis was assessed by Sirius red staining for collagen fibers in sections of the left ventricle of the heart of WT and PAD4$^{-/-}$ retired breeders (12–17 mo). The percentage of fibrotic (red) area in the heart tissue was quantified by ImageJ, excluding perivascular fibrosis. In PAD4$^{-/-}$ retired breeders, there was significantly less interstitial fibrosis than in WT retired breeders; $n = 6$. (B) The same analysis was performed for young (6–8 wk) WT and young PAD4$^{-/-}$ mice as well as for old (14–18 mo) WT and old PAD4$^{-/-}$ mice on standard diet. Quantification of Sirius red staining again showed less fibrosis in the old PAD4$^{-/-}$ mice compared with the old WT mice. In old PAD4$^{-/-}$ mice, the percentage of interstitial collagen remained comparable with young PAD4$^{-/-}$ mice; $n = 7$–8. (C and D) Representative Sirius red (left; collagen fibers are red) and Masson's trichrome (right; collagen fibers are blue) staining in young (C) and old (D) WT or PAD4$^{-/-}$ mice. Arrowheads point to interstitial collagen fibers. (E) Representative immunofluorescent staining for type I collagen in old WT or PAD4$^{-/-}$ mouse hearts. Bars: (C and D) 100 µm; (E) 10 µm. (F) Correlation analysis including all experimental groups between the degree of fibrosis (%) as determined by Sirius red staining, and ejection fraction (EF; %; Spearman r coefficient = −0.42, P = 0.014). *, P < 0.05; **, P < 0.01 by Mann–Whitney U test (A and B) or nonparametric correlation analysis (F). The graphs show mean and SEM from six (A, C, and D), seven to eight (B), or four (E) mice per group from two independent experiments. F shows a correlation analysis of all experimental groups from A and B.

assessed by Masson's trichrome stain (Fig. 5 A) and confirmed by hydroxyproline assay in lung homogenates (Fig. 5 B).

In the old mice on standard laboratory diet, the difference between genotypes was also highly significant (Fig. 5, C and D). Compared with young mice, both WT and PAD4$^{-/-}$ old mice showed an age-related increase in collagen deposition in the lung (Fig. 5 D). However, in the WT mice, this increase was more pronounced. Therefore, the age-related fibrosis was in part dependent on PAD4 expression. Respiration exposes the airways of the lung to the outside world, and minor infections or inhalation of particulate matter may contribute to injury, leading to fibrosis. However, PAD4 deficiency significantly reduced fibrosis in aging lungs.

Thus, our data show that aging is associated with an increase of interstitial fibrosis in different organs as determined by two different histochemical stains for collagen and confirmed by immunofluorescent staining. PAD4$^{-/-}$ mice were, to a great degree, protected from this age-associated fibrosis.

PAD4 mRNA expression is low in heart and lung tissue

As the mice we are studying are PAD4 null in all cells, we sought to better understand the level of PAD4 expression in

Downloaded from http://rupress.org/jem/article-pdf/214/2/439/1756691/jem_20160530.pdf by guest on 08 February 2026

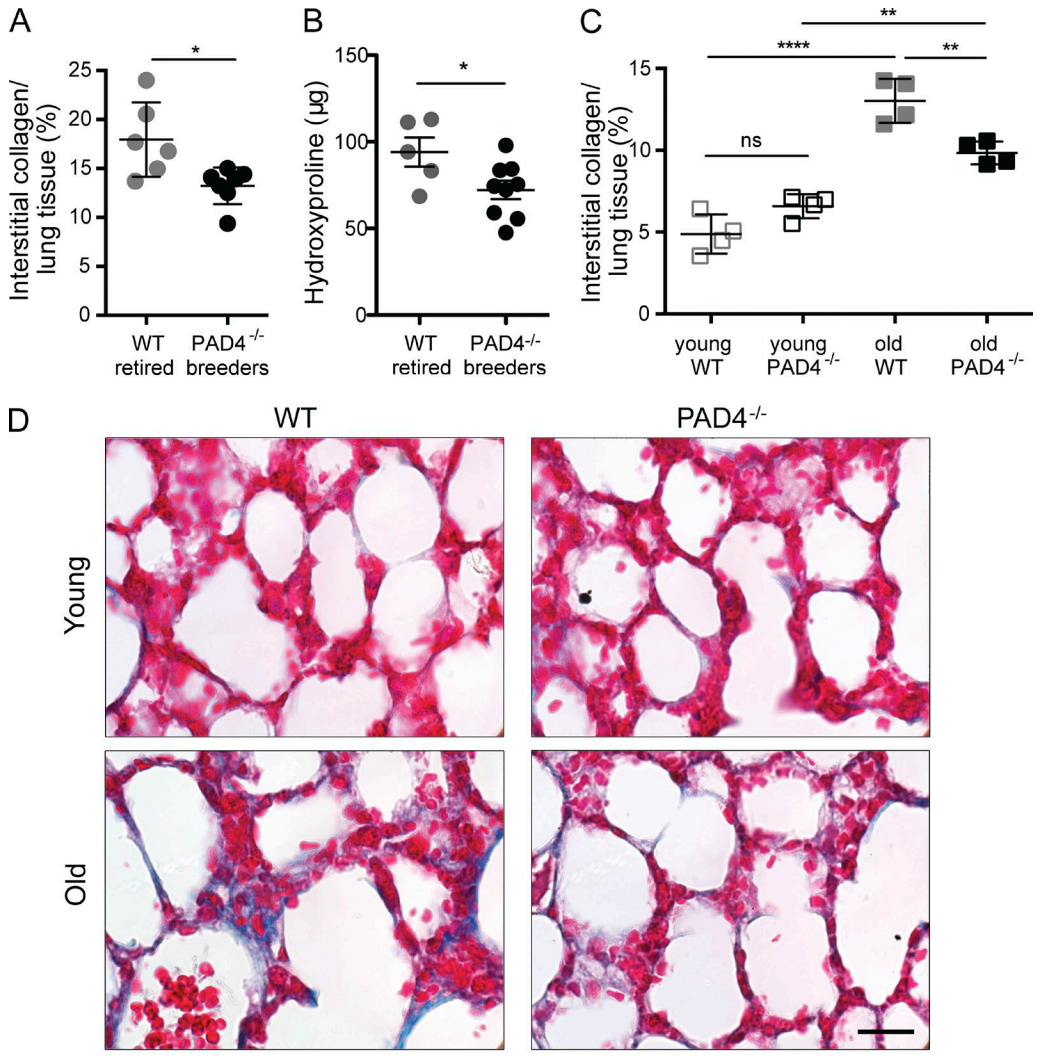

Figure 5. **Old PAD4$^{-/-}$ mice have significantly less collagen staining in their lungs than old WT mice.** (A) The percentage of collagen-positive area in lung tissue of WT and PAD4$^{-/-}$ retired breeders (12–17 mo) was quantified using Masson's trichrome stain for collagen and subsequently color gating for blue fibers; n = 6–7. (B) Measurement of hydroxyproline content in the right lung was performed; n = 5–9. (C) The same analysis as in A for collagen fibers within the lung tissue was performed for young (6–8 wk) WT and PAD4$^{-/-}$ mice and old (14–18 mo) WT and PAD4$^{-/-}$ mice; n = 4. (D) Representative photographs of lung sections stained with Masson's trichrome stain are shown. Bar, 20 µm. *, P < 0.05; **, P < 0.01; ****, P < 0.0001 by Mann–Whitney U test. The graphs show mean and SEM from six to seven (A), five to nine (B), or four (C and D) mice per group from three (A), one (B), or two (C and D) independent experiments.

different organs. PAD4 is highly expressed in granulocytes but may also be expressed to some level in many tissues (Asaga et al., 2001; van Beers et al., 2013) and is up-regulated in various tumors (Chang and Han, 2006). We performed quantitative real-time PCR analysis and found that PAD4 mRNA levels were high in tissues with abundant neutrophils, including bone marrow and spleen (Fig. 6 A), but also in colon, skin, and thymus. In comparison, liver, heart, and lung had relatively little to no expression of PAD4 (Fig. 6, A and B), comparable to background of PAD4$^{-/-}$ bone marrow. Therefore, we consider it unlikely that intrinsic PAD4 expression within the cells of the heart or lung is responsible for the fibrotic changes we saw in these organs with age. We compared PAD4 mRNA expression in aged animals and found a slight increase in old animals in lung tissue but not in the heart (Fig. 6 C). We also did not observe a significant increase in PAD4 mRNA expression in isolated neutrophils from young or old mice (Fig. 6 C). Hence, an increase in this gene's transcription was not responsible for the elevated NETosis seen in isolated neutrophils from old mice in vitro.

DNase administration and PAD4 deficiency similarly protect from cardiac damage in the pressure-overloaded heart

Although expression of PAD4 is very low in the heart (Fig. 6), we wanted to convince ourselves that extracellular chromatin generated by PAD4 activity actually induces fibrosis. However,

Downloaded from http://rupress.org/jem/article-pdf/214/2/439/1756691/jem_20160530.pdf by guest on 08 February 2026

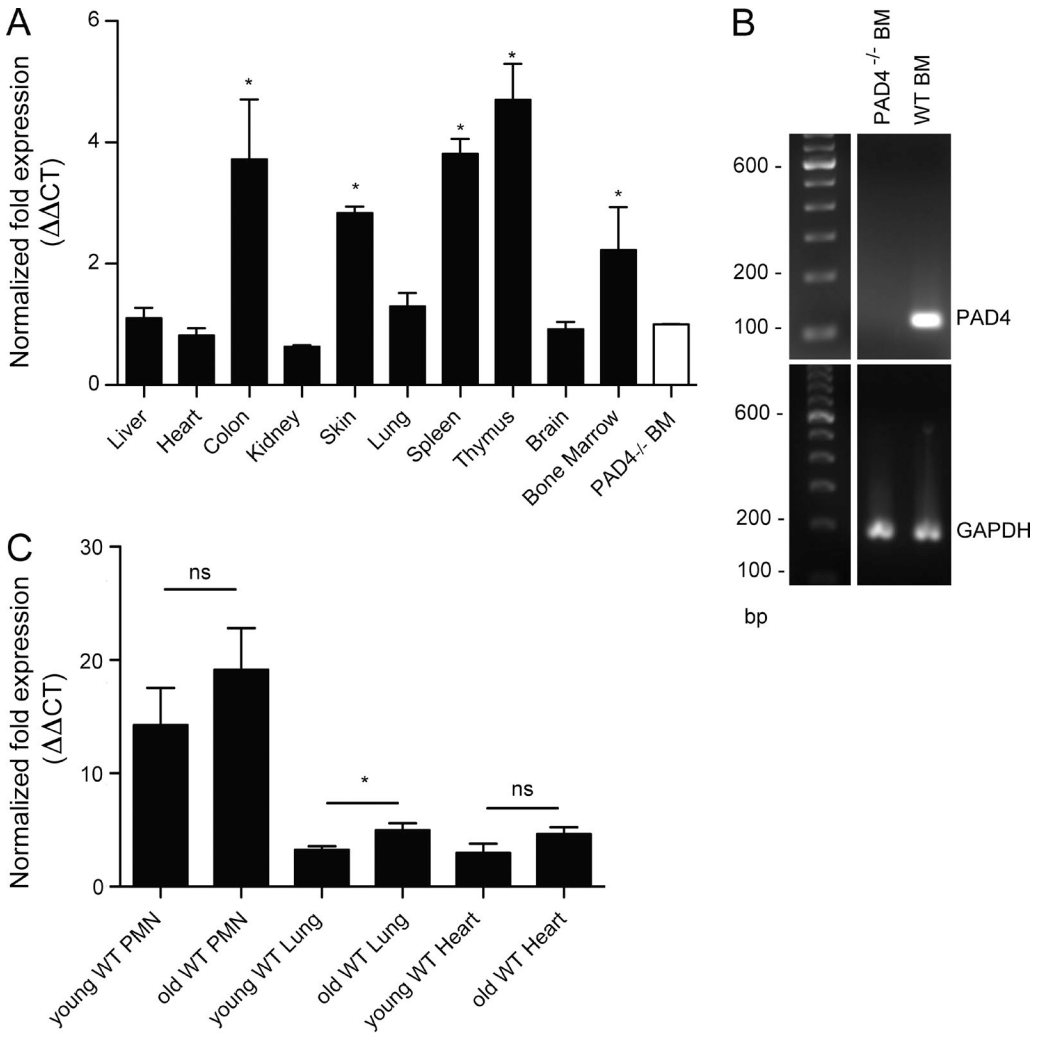

Figure 6. **Cardiac and lung tissue have low PAD4 mRNA expression compared with other organs in young and old mice.** (A) Quantitative real-time RT-PCR analysis was performed for PAD4 mRNA expression in various tissue types from WT mice. Fold expression was calculated with actin B and hypoxanthine-guanine phosphoribosyltransferase (*hprt*) as reference genes and normalized to PAD4$^{-/-}$ bone marrow; $n = 5$. (B) PCR product size and specificity after amplification was verified by conventional PCR on an agarose gel. A representative photograph is shown. (C) Quantitative real-time PCR analysis of PAD4 mRNA expression in young (2 mo) compared with old (20–25 mo) WT C57BL/6NIA mice. Fold expression was calculated with *gapdh* and *hprt* as reference genes and normalized to PAD4$^{-/-}$ bone marrow; $n = 5$. *, $P < 0.05$ by Student's *t* test. The graphs show mean and SEM from five (A and C) or three (B) mice per group from two independent experiments.

identifying NET formation that may occur intermittently during the aging process is not experimentally feasible. We therefore opted to study a classic model of heart fibrosis, ascending aortic constriction (AAC), which results in heart failure and myocardial fibrosis in young animals (Tarnavski et al., 2004), using 2-mo-old WT and PAD4$^{-/-}$ mice. In parallel, a group of WT mice subjected to AAC was treated with DNase 1, which promotes the clearance of extracellular chromatin, such as that produced by NETosis (Hakkim et al., 2010).

Invasion of inflammatory cells into the perivascular myocardial tissue has been observed shortly after induction of aortic stenosis in mice (Weisheit et al., 2014), but NETosis has not been examined in this model. To do this, we subjected a group of WT or PAD4$^{-/-}$ mice to AAC for 1 d, digested the hearts, and analyzed infiltrating CD45^{+} leukocytes by flow cytometry (Hilgendorf et al., 2014). A significantly elevated number of neutrophils (CD11b^{+}Ly6G^{+} cells; Fig. 7 A) and NETting (undergoing NETosis) neutrophils (Ly6G^{+}H3Cit^{+}; Fig. 7 B; Gavillet et al., 2015) were identified in the hearts of WT but not PAD4$^{-/-}$ mice that had undergone AAC compared with sham-operated controls. As this flow cytometric approach requires some processing time that could be allowing for ex vivo NET formation, we also analyzed snap-frozen tissue for the presence of NETs by histology in mice immediately perfused after euthanasia. In WT mice subjected to AAC, we identified extracellular H3Cit originating from Ly6G^{+}

Downloaded from http://rupress.org/jem/article-pdf/214/2/439/1756691/jem_20160530.pdf by guest on 08 February 2026

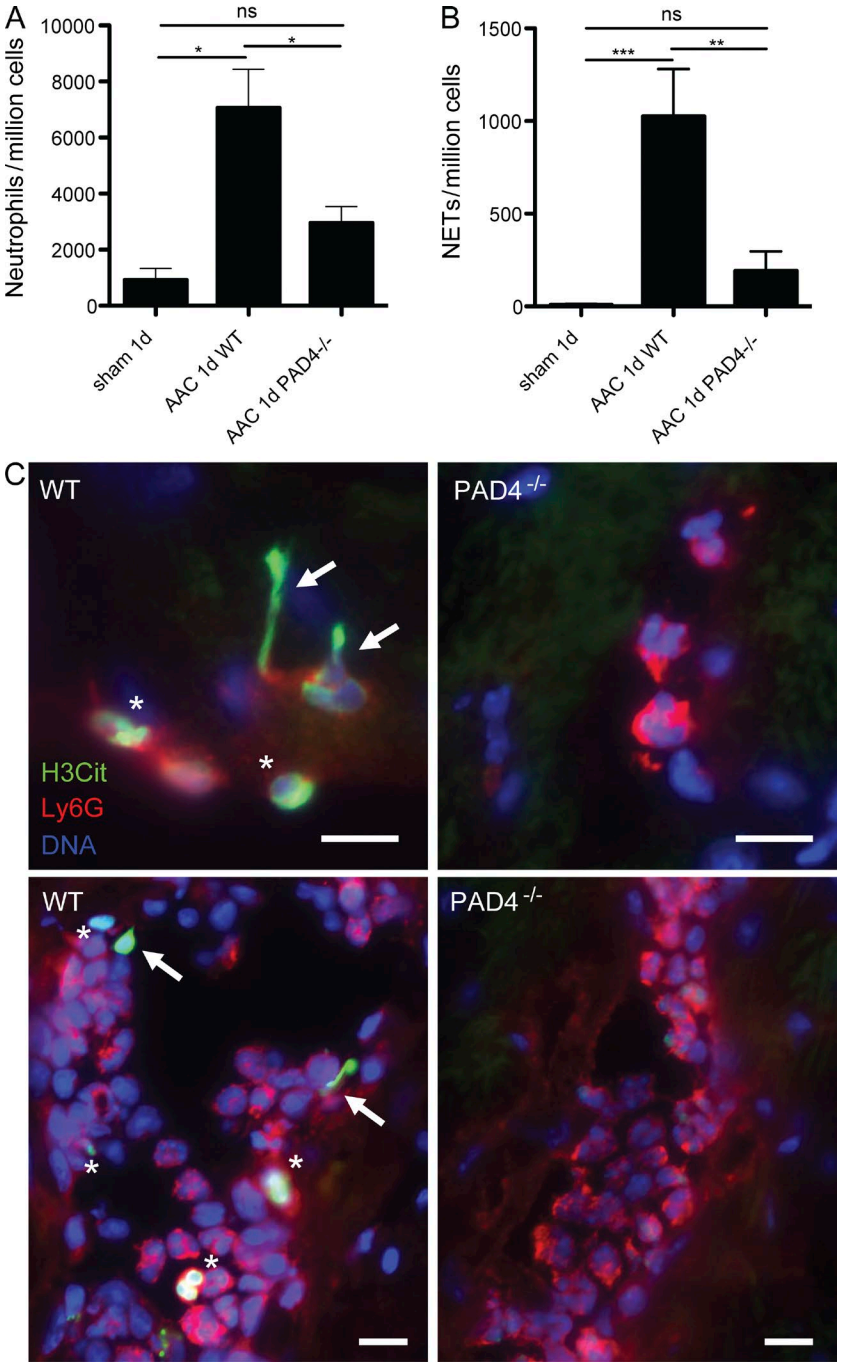

Figure 7. **NETosis occurs in the pressure-overload mouse model of cardiac fibrosis.** WT or PAD4$^{-/-}$ mice were subjected to AAC or to sham surgery, and 1 d later, cellular composition of the left ventricle was analyzed by flow cytometry. (A and B) Neutrophils were identified as CD45.2^{+}CD11b^{+}Ly6G^{+} cells (A), and neutrophils undergoing NETosis were identified within this gated population as H3Cit^{+} (B); n = 3–7. *, P < 0.05; **, P < 0.01; ***, P < 0.001 by Student's t test. (C) Representative immunofluorescence staining images. NETs (arrows) and hypercitrullinated histone H3 (H3Cit)–positive neutrophils (asterisks) were present in WT but not PAD4$^{-/-}$ hearts 1 d after AAC. Bars, 10 µm. The graphs show mean and SEM from three to seven mice per group in two independent experiments.

neutrophils (Fig. 7 C, arrows), as well as neutrophils in earlier stages of NETosis, where histone H3 is hypercitrullinated in nuclei (Fig. 7 C, asterisks). Neither was present in hearts of PAD4$^{-/-}$ animals that had undergone AAC (Fig. 7 C). This confirmed neutrophil recruitment and NETosis in the AAC model. This also showed that PAD4 was responsible for histone H3 citrullination, as other PAD enzymes are present in neutrophils and cells from cardiac tissue itself. These enzymes could have been released by the pressure overload and citrullinated extracellular chromatin originating from cell death other than NETosis. Flow cytometry showed that NETting neutrophils were still present, but fewer in number, at 3 d after AAC in WT hearts (neutrophils: AAC, 2,939 ± 353.4, n = 5; sham-operated, 198.1 ± 40.5, n = 4; P = 0.0003; NETs: AAC, 569.8 ± 114.3, n = 5; sham, 69.5 ± 38.6, n = 4; P = 0.007). Therefore, NET formation occurs transiently in this model that is dependent on recruitment of inflammatory cells.

It has been reported that platelets are the main source of fibrosis-promoting TGFβ in a similar aortic constriction model (Meyer et al., 2012), and NETs recruit platelets (Fuchs

Downloaded from http://rupress.org/jem/article-pdf/214/2/439/1756691/jem_20160530.pdf by guest on 08 February 2026

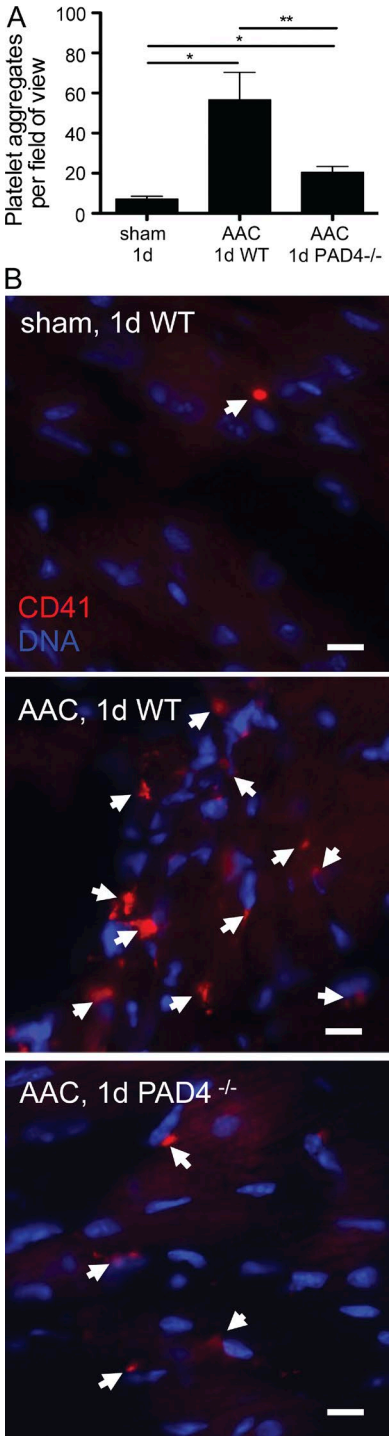

Figure 8. **Platelet aggregates form within AAC hearts to a greater extent in WT than PAD4$^{-/-}$ mice.** (A) Quantification of platelet aggregates (CD41-positive staining) in mice subjected to AAC or a sham operation and perfused immediately after euthanasia. Five fields of view were imaged and analyzed per heart section using a 10× objective; $n = 3–7$. *, $P < 0.05$; **, $P < 0.01$ by Student's t test. (B) The top panel shows a representative image of sham-operated WT mouse heart immunostained with anti-CD41 antibody to identify platelets. The middle and bottom panels show representative images of the relative presence of CD41$^+$ platelet aggregates (arrows) in WT hearts compared with PAD4$^{-/-}$ hearts. Bars, 10 µm. The graph shows mean and SEM from three to seven mice per group in two independent experiments.

et al., 2010). We were therefore interested in assessing the platelet response and recruitment in this model. By immunostaining for the platelet-specific integrin αIIb (CD41), we identified areas of platelet accumulation in the hearts of perfused mice by histology, which we quantified (Fig. 8 A). Both WT and PAD4$^{-/-}$ mice had an elevation in platelet aggregates compared with sham mice. However, WT hearts recruited significantly more platelets than PAD4$^{-/-}$. Representative images are shown in Fig. 8 B. Thus, a lack of NETs in PAD4 deficiency may be attenuating platelet accumulation in this model and with it local TGFβ production.

We next wished to assess the long-term effect of PAD4 deficiency or DNase treatment in the AAC model. WT and PAD4$^{-/-}$ mice underwent AAC and were injected with saline for 7 d. In parallel, a set of WT mice underwent AAC but were injected with rhDNase 1 for 7 d to degrade NETs. We evaluated heart structure and function by echocardiography for 4 wk. PAD4$^{-/-}$ mice were protected from the decline in LVEF seen in WT mice at early (3 and 7 d) and also late (28 d) time points (Fig. 9 A). rhDNase 1–treated mice had an initial decline in LVEF at days 3 and 7. By 28 d, these mice had significantly improved LVEF compared with WT mice treated with saline, and LVEF was not different from PAD4$^{-/-}$ mice (Fig. 9 A). For reference, LVEF values for sham-operated animals are depicted in gray at the respective time points. Structural parameters were unchanged among groups (Fig. 9, B–D).

Collagen content was assessed histologically using Masson's trichrome stain after 28 d (Fig. 9 E), a time sufficient for development of cardiac fibrosis in this model (Namba et al., 1997). Quantification of the stained tissue sections revealed that although WT mice had substantial collagen deposition, PAD4$^{-/-}$ mice or DNase-treated mice had only focal traces of collagen in the interstitial space of the myocardium (Fig. 9 F). The presence of collagen was similarly low in PAD4$^{-/-}$ mice and DNase 1–treated WT mice, within the range of sham-operated WT animals in both groups. PAD4$^{-/-}$ mice also had significantly less perivascular fibrosis than WT mice (Fig. 9 G). Of note, perivascular fibrosis does not generally correlate with either interstitial fibrosis or ejection fraction in patients with nonischemic heart failure (Dai et al., 2012).

Collectively, these results indicate that PAD4 and extracellular DNA contribute to the deposition of collagen in this experimental model of cardiac fibrosis. Because the presence of extracellular DNA/chromatin participated in the induction of collagen deposition in this model, it is more likely that PAD4-mediated NETosis rather than PAD4-mediated changes in gene transcription were responsible. The presence of PAD4 also enhanced neutrophil and platelet recruitment, which may increase inflammatory collateral damage and TGFβ delivery, thus promoting fibrosis.

Downloaded from http://rupress.org/jem/article-pdf/214/2/439/1756691/jem_20160530.pdf by guest on 08 February 2026

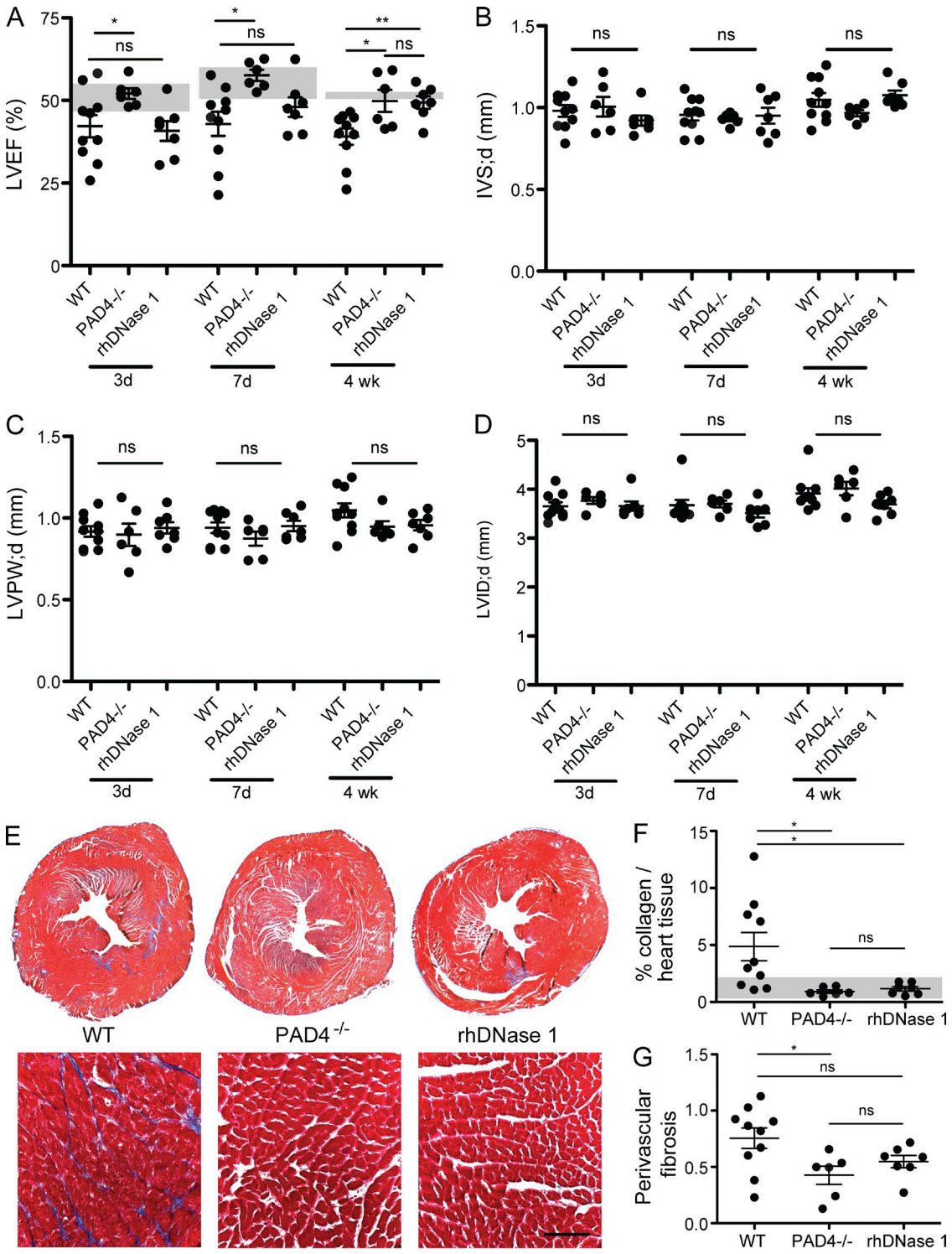

Figure 9. **Extracellular DNA/PAD4 contribute to cardiac damage in the pressure-overloaded heart.** WT and PAD4$^{-/-}$ mice were subjected to AAC and underwent echocardiography 3, 7, or 28 d after surgery. Mice received either vehicle or rhDNase 1 administration every 12 h for the first 7 d. (A) LVEF measurements in WT, PAD4$^{-/-}$, or rhDNase 1–treated mice. Range of ejection fraction values (n = 4) from sham-operated animals at each respective time point are shown in gray. The structural parameters IVS;d (B), LVPW;d (C), and LVID;d (D) were similar between all groups. (E–G) Mice were euthanized 28 d after AAC induction for fibrosis analysis. (E) Representative composite images (top) or high magnification (bottom) of the left ventricle stained with Masson's trichrome. Bar, 100 µm. (F) Quantification of interstitial fibrosis in images of Sirius red–stained heart tissue; n = 6–11. The range of values for per-

Downloaded from http://rupress.org/jem/article-pdf/214/2/439/1756691/jem_20160530.pdf by guest on 08 February 2026

DISCUSSION

In older persons, the balance between innate immunity and adaptive immunity shifts toward innate immunity, with a decrease in lymphocytes that may be accompanied by an increase in neutrophil counts (Cakman et al., 1996; Schröder and Rink, 2003). We saw increases in both neutrophil and platelet counts in our aged animals, as well as in platelet–neutrophil complexes. Moreover, activation of platelets through TLR4 or thrombin receptors and their subsequent interactions with neutrophils stimulate NETosis in mice (Clark et al., 2007; Etulain et al., 2015). Therefore, a NET-inducing trigger could be further propagated by the increased platelet count, and increased platelet recruitment by NETs could promote fibrosis via TGFβ release (Meyer et al., 2012).

In our study, the propensity of neutrophils from older mice for PAD4-mediated histone citrullination and NET formation was significantly elevated compared with young mice after exposure to PMA, a ROS-dependent inducer of NETosis, or ionomycin, a ROS-independent inducer of calcium influx and PAD4 activation (Parker et al., 2012). This neutrophil priming by aging was clearly seen even without stimulation, as neutrophils from aged mice had higher baseline values of H3Cit and produced more NETs after isolation. We determined this in two independent strains of C57BL/6 mice: C57BL/6J and C57BL/6NIA. To our knowledge, priming for NETosis of peripheral blood neutrophils in an aging host has not been previously observed. Interestingly, it was recently reported that older neutrophils in the bloodstream have a more proinflammatory phenotype with enhanced NET formation (Zhang et al., 2015), which raises the question whether this population may be increasing in aging individuals.

In spite of their proposed protective role in infectious diseases (Brinkmann et al., 2004), NETs and their components are cytotoxic, proinflammatory, and prothrombotic (Xu et al., 2009; Fuchs et al., 2010; Demers et al., 2012). Elevated levels of NETs or their biomarkers are associated with several noninfectious diseases such as autoimmune disease (Kessenbrock et al., 2009; Hakkim et al., 2010; Dwivedi et al., 2012), arteriosclerosis (Borissoff et al., 2013; Quillard et al., 2015), cancer (Demers et al., 2012), deep vein thrombosis (Brill et al., 2012; Diaz et al., 2013), and myocardial infarction (Savchenko et al., 2014a), all of which present a growing challenge to the health care system as the incidence of these diseases increases dramatically with population age. In many cases, NETs contribute to the disease process or its complications. Therefore, these could be exacerbated by excessive NETosis in aging animals and possibly humans.

Excessive NETosis may also impact organ function, such as that of the heart. Understanding the mechanisms leading to age-related organ dysfunction is essential for providing adequate care for our rapidly aging population. Aging can cause myocardial damage via excessive ROS production by mitochondria-rich cardiomyocytes (Dai and Rabinovitch, 2009), and extracellular ROS augment neutrophil–endothelial interactions (Patel et al., 1991). We have shown in an acute model of myocardial ischemia/reperfusion (MI/R) injury (Savchenko et al., 2014a) and now also in the aortic constriction model of cardiac pressure overload that extracellular chromatin is injurious to the heart and detrimental to its function. We were thus interested if in old age, where we saw priming for NETosis, heart function could be affected. To approach this, we used PAD4$^{-/-}$ mice, which are deficient in NETosis. Interestingly, we observed a significant difference between both the systolic and the diastolic functional measurements in old WT versus old PAD4$^{-/-}$ mice. WT mice had an expected age-related decline in heart function (Dai and Rabinovitch, 2009), with values very similar to those previously reported in the literature (Yang et al., 1999). Surprisingly, heart function in the old PAD4$^{-/-}$ mice remained comparable to that of young mice, both for systolic (LVEF) as well as diastolic (E/A ratio) parameters. Therefore, the aging mouse heart could be undergoing chronic injury caused by interstitial NET formation over time, negatively affecting heart function, particularly in the old mice. NETs and NET-mediated collateral injury may recruit platelets and help to initiate and propagate chronic inflammatory processes, consequently accelerating the onset of aging. The old heart may reflect the life history of insults during which NETs were produced and left a scar. Interestingly, there is increasing evidence that childhood infections (that could induce NETs) may cause health problems in adulthood and in old age (Bengtsson and Lindstrom, 2003; Finch and Crimmins, 2004; National Institute on Aging, 2011). Thus, an infection may initiate an injury that will be aggravated by aging.

We assessed interstitial fibrosis in old and young WT mice. We found an increase in interstitial fibrosis in the old WT mice. Nevertheless, such an age-related increase was reduced (in the lung) or absent (in the heart) in old PAD4$^{-/-}$ mice. Although collagen and other ECM components play an important role in maintaining tissue integrity and provide "healthy signaling," it is likely that excessive ECM accumulation reduces ventricular compliance and impairs cardiac function, both diastolic and systolic (Biernacka and Frangogiannis, 2011), as we have seen in the old WT mice. The extent of interstitial fibrosis observed in aged hearts correlated inversely with LVEF, indicating that indeed myocardial fibrotic changes are a relevant factor in age-related functional decline.

Different organs may be differentially affected by PAD4 deficiency. In the lung, the age-related fibrosis we observed was only in part dependent on PAD4 expression. However,

centage of collagen in sham-operated animals is represented by the gray-shaded area. (G) Perivascular fibrosis, quantified as the ratio of collagen-positive area to total vessel area. At least eight vessels were quantified per mouse; $n = 6–11$. *, $P < 0.05$; **, $P < 0.01$ by Student's t test. The graphs show mean and SEM from $n = 4–11$ mice per group from three independent experiments.

Downloaded from http://rupress.org/jem/article-pdf/214/2/439/1756691/jem_20160530.pdf by guest on 08 February 2026

even in the old lungs, PAD4 deficiency significantly reduced fibrosis, which might lead to improved lung performance. A recent study (Chrysanthopoulou et al., 2014) showed that NETs promoted differentiation of lung fibroblasts in culture into a myofibroblast phenotype, which increased connective tissue growth factor expression, collagen production and fibroblast proliferation/migration. NETs may similarly modify the cellular behavior in vivo, thus promoting fibrosis. Furthermore, neutrophil elastase, a protease that is released along with NETs with its activity maintained (Kolaczkowska et al., 2015), has been shown to directly contribute to lung fibrosis after bleomycin-induced lung injury (Chua et al., 2007). One could speculate that reduction of NETosis by PAD4 inhibition or destruction of NETs by DNase during a major lung infection or after a lung injury might prevent the initiation of future chronic fibrotic disease.

The striking reduction of interstitial collagen in PAD4$^{-/-}$ mice and the protection from heart malfunction raised the question as to why PAD4$^{-/-}$ mice would be protected from fibrosis in old age. Apart from its role in histone hypercitrullination during NETosis, PAD4 is involved in gene expression by regulating histone methylation (Wang et al., 2004). We have now shown that PAD4 is only weakly, if at all, expressed in cardiac tissue. Together with our results with DNase 1 infusion in the AAC model showing that it is extracellular DNA that promotes fibrosis, we think that in the fibrotic process, PAD4 regulates NETosis. This does not exclude that there could be contributing changes in gene expression in the organ tissue itself caused by PAD4 deficiency, especially in aged mice. PAD4, through demethylation of histone arginines, has been shown to repress p53 target gene expression (Li et al., 2008), and thus, its deficiency could have further effects in aging that should be investigated. One of the main regulators of fibrosis is TGFβ. Platelets are a significant source of TGFβ, and NETs promote recruitment and activation of platelets (Fuchs et al., 2010). The finding that more platelets express TGFβ with the same stimulus in old WT mice is also intriguing in this context.

In the experimental cardiac fibrosis model, it is important to distinguish between changes in function at early versus late time points, as fibrosis develops only after 10–14 d (Higashiyama et al., 2007). We believe that in the first week, the heart undergoes functional changes through NET toxicity and microvessel dysfunction because of the initial pressure overload injury/inflammation. This inflammation is likely directly damaging cardiomyocytes, leading to poor function early on. As we show, inflammation decreases after that, but then the fibrotic response to the inflammation/injury develops, keeping heart function down at day 28. Therefore in a fully resolved acute inflammatory response, ejection fraction could theoretically recover if the heart remodeled back to its original state. In WT mice, however, this remodeling is impaired by excessive ECM/collagen deposition, and therefore, function either continues to decline or remains lowered to 28 d. PAD4$^{-/-}$ mice have less initial inflammation, and thus, their heart is protected early and also late because they are protected from excess interstitial and perivascular collagen deposition. It appears that never forming NETs (as with PAD4 deficiency) is better for the heart in the first week of AAC than clearing them once already formed with DNase. However, digestion of NETs with DNase helps to prevent long-term fibrosis to a similar extent as not expressing PAD4 (day 28).

Chronic elevation of NET components in tissue may lead to repeated injury and the formation of excess matrix. Indeed, polymorphisms in DNase 1 within the human population resulting in a decrease of activity (and therefore a defect in NET degradation) are associated with an increased risk of myocardial infarction (Kumamoto et al., 2006). It is possible that reduced DNase 1 activity may promote organ fibrosis, whereas elevation of DNase 1 is protective. The NET-inducing events that might contribute to organ dysfunction include hypoxia, mechanical injury, and various types of infections. As humans are much more exposed to such stressors than mice living in a protected specific pathogen–free environment, one would expect the unfavorable effects of life to be of even more consequence in humans than in laboratory mice.

Our study on aging in mice suggests that limiting PAD4 activity and excessive NET production in known NET-inducing conditions, especially in old age, could be beneficial. This could be especially relevant in acute situations leading to myocardial injury by infection, such as myocarditis and septic cardiomyopathy, or by elevated heart strain as it occurs in hypertensive crisis, myocardial infarction, and pulmonary embolism. Acute events leading to respiratory distress and detrimental NET production such as transfusion-related acute lung injury (Caudrillier et al., 2012; Thomas et al., 2012) or secondary infections accompanying influenza (Pillai et al., 2016) may also benefit. In addition to these rather severe settings, the sum of minor injuries, such as by respiratory infections, over a lifetime may lead to a fibrotic condition. NET-targeted therapeutics could involve digesting NETs with DNases, inhibiting their formation with PAD4 inhibitors or neutralizing their toxic components, such as histones or elastase (Xu et al., 2009; Martinod and Wagner, 2014). These short-term treatments may have positive long-term effects on organ function, and perhaps even on longevity of individuals, and thus their investigation is worth pursuing.

MATERIALS AND METHODS

Animals

20–27-mo-old C57BL/6NIA mice for in vitro NETosis studies were obtained from the Aged Rodent Colony of the National Institute on Aging of the National Institutes of Health, maintained at Charles River Laboratories. Young mice (8–16 wk old) for these experiments were obtained from the same colony.

PAD4$^{-/-}$, originally generated by Y. Wang (Pennsylvania State University, College Park, PA), and correspond-

Downloaded from http://rupress.org/jem/article-pdf/214/2/439/1756691/jem_20160530.pdf by guest on 08 February 2026

ing WT mice were on a C57BL/6J background. Retired breeders had been kept on LabDiet PicoLab Mouse Diet 20, which is fortified with a higher fat content for growth and reproduction (21.635% calories provided by fat), from 6–10 wk of age until the time of sacrifice. Nonbreeders and all young mice were kept on a standard laboratory diet (LabDiet Prolab IsoPro RMH 3000, 14.276% calories provided by fat) throughout their life. Young animals were 6–8 wk old, retired breeders were 12–17 mo old, and old mice that had been kept on standard laboratory diet were 14–18 mo old. The old mice used for the diastolic measurements were 18 mo old for the PAD4$^{-/-}$ mice and between 15 and 20 mo old for the old WT mice, whereas young mice in this experiment were 8 wk old.

All groups were age and sex matched and were fed ad libitum with free access to water. All experimental procedures were reviewed and approved by the Institutional Animal Care and Use Committee of Boston Children's Hospital (protocol nos. 14-03-2631R and 14-02-2609R).

Analysis of peripheral blood and cytospin

Blood was collected from anesthetized mice via the retroorbital sinus into EDTA-coated capillary tubes and was analyzed by a Hemavet 950FS (Drew Scientific) for complete blood counts.

25 µl whole blood was incubated in ACK (ammonium chloride potassium) lysis buffer for 10 min on ice and then cytocentrifuged using a Statspin Cytofuge 2. Samples were immediately fixed in 4% paraformaldehyde for 2 h at room temperature and then immunostained for H3Cit and Ly6G (clone 1A8) as previously described (Demers et al., 2012). Images were acquired of cells from 10–15 fields of view at 200 magnification using a ZEISS Axiovert 200m inverted epifluorescence microscope and ZEISS AxioVision software. Thresholding analysis was performed using ImageJ software (National Institutes of Health) to calculate the population of H3Cit-positive neutrophils in each sample.

Peripheral blood neutrophil isolation and NET induction

Peripheral blood neutrophils were isolated as described previously (Demers et al., 2012) and stimulated with 4 µM calcium ionophore or 100 nM PMA for 3.5 h. Cells were fixed with 2% (vol/vol) paraformaldehyde, and DNA was stained with Hoechst 33342 (Invitrogen) for visualization of NETs using an epifluorescent Axiovert microscope (ZEISS). NETs were counted from five distinct fields of view in triplicate wells and expressed as percentage of NET-forming cells per total number of cells in the field.

Pulse oximetry

Peripheral capillary oxygen saturation was measured under conscious condition in mice that were previously trained to wear neck collars. This was done using the rodent pulse oximeter sensor Mouse Ox system (Starr Life Sciences), and a mean value over 10 min was used for analysis.

Echocardiography

Cardiac function and heart dimensions were measured as described previously (Savchenko et al., 2014a). The M-mode was used to evaluate left ventricular internal dimension (LVID), left ventricular interventricular septum (LVIS), and left ventricular posterior wall thickness (LVPW) at end diastole and end systole. Echocardiograms were stored digitally, and ejection fraction (LVEF; percentage of blood volume ejected from the left ventricle with each heartbeat) was calculated using Vevostrain software. Flow pattern across the mitral valve was measured in the four-chamber view using the pulsed wave (PW) Doppler mode to determine evidence of impaired ventricular relaxation. Ventricular filling pattern is expressed as the ratio between the E and the A wave (E/A).

Blood pressure measurements

Systolic blood pressure was measured using an IITC 12M22931 noninvasive blood pressure system (IITC Life Science). Mice were trained twice several days before the measurements to accustom them to measurement conditions. For measurements, the mice were placed into restrainers and allowed to settle down for 10 min. Systolic blood pressure was determined by the tail cuff in a chamber at 34°C. Blood pressure was measured five times, and the mean of the obtained values is presented.

Histology

Anesthetized mice were sacrificed by cervical dislocation, and lungs and hearts removed and preserved in 10% neutral buffered formalin solution for at least 24 h. Organs were embedded in paraffin, sectioned, and rehydrated. To assess collagen content in heart tissue, Sirius red staining solution was prepared with 0.5 g Direct Red 80 (Sigma-Aldrich) powder in 500 ml of a saturated aqueous solution of picric acid (Sigma-Aldrich). Sirius red stains collagen I, II, and III by reacting, via its sulfonic acid groups, with basic groups of the collagen molecule (Junqueira et al., 1979). Slides were stained for 60 min, washed twice in acidified water (5% vol/vol acetic acid), dehydrated, and mounted using a resinous mounting medium. At least five photographs of left ventricular heart tissue were taken at 250 magnification in bright-field microscopy in a blinded manner. The content of red fibers (collagen) per section was determined using ImageJ software, perivascular fibrosis was excluded from the calculation. We confirmed the presence of collagen with polarized light filters to visualize birefringence. A subset of slides was stained with Weigert's hematoxylin before Sirius red staining and was used for the generation of representative pictures of heart tissue. For quantification, slides without nuclear staining were used to avoid interference of hematoxylin with the quantification algorithm. Mosaics of representative areas of the left ventricle were generated using the MosaicJ plugin of ImageJ (Thévenaz and Unser, 2007). For trichrome staining of lung tissue, the Masson trichrome stain kit (Sigma-Aldrich) was used according to the manufacturer's protocol. Nuclei were not stained with hematoxylin to avoid interference with

Downloaded from http://rupress.org/jem/article-pdf/214/2/439/1756691/jem_20160530.pdf by guest on 08 February 2026

the quantification of collagen content. For quantification, at least six photographs of lung parenchyma or 10 images of myocardium were taken by bright-field microscopy by an investigator blinded to the identity of the samples. The area of blue fibers (collagen) per lung tissue (excluding empty alveolar spaces) or cardiac tissue was calculated using ImageJ software.

Hydroxyproline assay

Hydroxyproline was quantified by a previously described method with slight modification (Woessner, 1961). In brief, homogenates of right lung were incubated with 12 N HCl for at least 16 h at 120°C. Clear supernatant obtained by centrifugation at 16,200 *g*, 15 min was mixed with citrate buffer (0.24 M citric acid monohydrate, 0.2 M acetic acid glacial, 0.53 M sodium acetate trihydrate, and 0.85 M sodium hydroxide) followed by incubation with chloramine T solution for 20 min at room temperature. Ehrlich's solution was added to the mixture and incubated for 20 min at 65°C. The absorbance was measured at 530 nm.

RT-PCR

Euthanized mice were immediately perfused with PBS before organ harvest. Total RNA was prepared from tissue using TRIzol extraction (Invitrogen) followed by an RNeasy micro kit with on-column DNase digestion (QIAGEN). cDNA was prepared using the Omniscript Reverse Transcription kit (QIAGEN) according to manufacturer's instructions. Quantitative real-time PCR was performed using Power SYBR Green Master Mix (Applied Biosystems) using a Bio-Rad Laboratories CFX Connect Real-Time PCR Detection System. Conventional PCR was performed using HotStarTaq DNA polymerase (QIAGEN) and the product run on a 1.5% agarose gel. The following primers were used: PAD4 (forward: 5′-GGCTACACAACCTTCGGCAT-3′, reverse: 5′-GCTGCTTTCACCTGTAGGGT-3′), actin B (forward: 5′-CTAAGGCCAACCGTGAAAAG-3′, reverse: 5′-ACCAGAGGCATACAGGGACA-3′), hprt (forward: 5′-GTTGGATACAGGCCAGACTTTGTTG-3′, reverse: 5′-GAGGGTAGGCTGGCCTATTGGCT-3′, gapdh (for quantitative PCR, forward: 5′-GGGGCTGGCATTGCCCTCAACG-3′, reverse: 5′-GGGGCTGGTGGTCCAGGGGT-3′; for conventional PCR, forward: 5′-CCATGGAGAAGGCTGGGG-3′, reverse: 5′-CAAAGTTGTCATGGATGACC-3′). Quantitative RT-PCR analysis was performed using the Livak method.

Immunofluorescence staining

Tissue was snap frozen in optimal cutting temperature medium. 10-µm cryosections were fixed in 2% paraformaldehyde, permeabilized with 0.1% Triton, blocked in 3% BSA, and incubated with the following primary antibodies overnight at 4°C: anti-CD41 (MWReg30; BD), anti-Ly6G (clone 1A8; BioLegend), anti-H3Cit (Abcam), and anti–type I collagen (Abcam). After washing, sections were stained with the respective Alexa Fluor–conjugated antibodies (Alexa Fluor 488 donkey anti–rabbit IgG and Alexa Fluor 555 goat anti–rat IgG; BioLegend) and counterstained with Hoechst 33342 (Invitrogen). Images were acquired using a ZEISS Axiovert epifluorescence microscope.

AAC model

Adult 9–10-wk-old male C57/BL6J mice (body weight, 25 ± 3 g) underwent either sham operation or AAC as described previously (Tarnavski et al., 2004). In brief, animals were anesthetized using 2–3% isoflurane, intubated, and ventilated using a small animal respirator (Harvard Apparatus). The chest was opened at the second to third intercostal space and the aortic arch visualized. A 25G needle was placed adjacent to the aorta, and a suture was tied around both the needle and aorta. In sham-operated animals, all surgical steps were performed except for this ligation. The needle was then removed, leaving a 25G opening in the aorta and resulting in significant stenosis. The chest was closed and the animal was weaned off the respirator as soon as spontaneous breathing had stabilized. Mice were treated intravenously by retroorbital injection with either 10 µg rhDNase 1 (Pulmozyme; Genentech) or sterile saline directly after extubation followed by intraperitoneal administration of 50 µg DNase 1 or the same volume of sterile saline every 12 h for the next 7 d. Continuous wave Doppler echocardiography was performed at 3, 7, and 28 d after surgery. All mice were sacrificed by an overdose of isoflurane followed by cervical dislocation at 28 d after surgery for tissue collection. A separate group of sham-operated animals were followed in the same manner and used to determine the range of LVEF and percentage of interstitial collagen values.

Assessment of NETting neutrophils by flow cytometry

Neutrophils were quantified in hearts that had undergone AAC or sham operation (1 or 3 d after surgery). Enzymatic digestion of heart tissue was performed as described previously (Hilgendorf et al., 2014). Neutrophils were labeled using PerCP-Cy5.5–conjugated anti-Ly6G (1A8) and APC-Cy7–conjugated anti-CD45.2 antibody (BioLegend). NETs were identified as described previously (Gavillet et al., 2015) as $H3Cit^+$ cells by immunofluorescent staining of non-permeabilized cell suspensions.

Flow cytometry analysis of platelet activation

50 µl of heparinized blood cells was washed twice in modified Tyrode-Hepes buffer (134 mM NaCl, 0.34 mM Na_2HPO_4, 2.9 mM KCl, 12 mM $NaHCO_3$, 5 mM Hepes, 1 mM $MgCl_2$, 5 mM glucose, and 0.35% BSA, pH 7.4) and diluted in Tyrode-Hepes buffer containing 2 mM $CaCl_2$. Samples were incubated with vehicle or a combination of 10 µM ADP (Chrono-Log) and 3 µM U46619 (Tocris Bioscience), stained for 8 min at 37°C and 7 min at room temperature with the fluorophore-labeled antibodies (FITC-CD41 [MwReg30], APC-TGFβ1, and Pacific Blue–Ly6G [1A8]; BioLegend) and analyzed on a FACSCanto (BD). Platelet–neutrophil

Downloaded from http://rupress.org/jem/article-pdf/214/2/439/1756691/jem_20160530.pdf by guest on 08 February 2026

complexes were identified as CD41-positive neutrophils and are expressed as percentage of total neutrophils. Gates were set for platelet–neutrophil complexes or TGFβ positivity based on comparison of the stimulated to unstimulated conditions in young WT mice.

Statistical analysis

Data are presented as means ± SEM. For statistical tests, a two-tailed Student's *t* test or Mann–Whitney *U* test was used when two groups were compared. For comparison of more than two groups, the one-way ANOVA with Bonferroni's post-test was applied. Correlation analysis was performed between the level of heart fibrosis and ejection fraction using Prism 6.0d software (GraphPad Software). All p-values <0.05 were considered significant.

ACKNOWLEDGMENTS

We thank Yanming Wang for sharing the PAD4$^{-/-}$ mice, Siu Ling Wong for helpful discussions, Lesley Cowan for assistance with manuscript preparation, and Christoph Bode and Daniel Dürschmied for their support during revisions. We are grateful for the animals obtained from the National Institutes of Health's NIA Aged Rodent Colony for this study.

This work was supported by the National Heart, Lung, and Blood Institute of the National Institutes of Health (grants R01HL102101 and R01HL125501 to D.D. Wagner and grant 5T32HL066987-13 to K. Martinod) and by a Boston Children's Hospital Research Faculty Council Award for Pilot Study (D.D. Wagner). L. Erpenbeck received a fellowship from the Deutsche Akademie der Naturforscher Leopoldina (Nationale Akademie der Wissenschaften). T. Witsch received a fellowship from the German Cardiac Society (Deutsche Gesellschaft fuer Kardiologie). D. Cherpokova received a fellowship from the Deutsche Forschungsgemeinschaft (CH 1734/1-1).

The authors declare no competing financial interests.

Submitted: 13 April 2016
Revised: 8 September 2016
Accepted: 7 December 2016

REFERENCES

Afonso, A.S., K.M. Verhamme, M.C. Sturkenboom, and G.G. Brusselle. 2011. COPD in the general population: prevalence, incidence and survival. *Respir. Med.* 105:1872–1884. http://dx.doi.org/10.1016/j.rmed.2011.06.012

Ammarguellat, F., I. Larouche, and E.L. Schiffrin. 2001. Myocardial fibrosis in DOCA-salt hypertensive rats: effect of endothelin ETA receptor antagonism. *Circulation.* 103:319–324. http://dx.doi.org/10.1161/01.CIR.103.2.319

Asaga, H., K. Nakashima, T. Senshu, A. Ishigami, and M. Yamada. 2001. Immunocytochemical localization of peptidylarginine deiminase in human eosinophils and neutrophils. *J. Leukoc. Biol.* 70:46–51.

Aw, D., A.B. Silva, and D.B. Palmer. 2007. Immunosenescence: emerging challenges for an ageing population. *Immunology.* 120:435–446. http://dx.doi.org/10.1111/j.1365-2567.2007.02555.x

Azevedo, E.P., A.B. Guimaraes-Costa, G.S. Torezani, C.A. Braga, F.L. Palhano, J.W. Kelly, E.M. Saraiva, and D. Foguel. 2012. Amyloid fibrils trigger the release of neutrophil extracellular traps (NETs), causing fibril fragmentation by NET-associated elastase. *J. Biol. Chem.* 287:37206–37218. http://dx.doi.org/10.1074/jbc.M112.369942

Bancroft, J., and M. Gamble. 2008. Connective tissue and stains. *In* Theory and Practice of Histological Techniques. J. Bancroft, editor. Churchill-Livingston Elsevier, London. pp. 135–160.

Beerman, I., D. Bhattacharya, S. Zandi, M. Sigvardsson, I.L. Weissman, D. Bryder, and D.J. Rossi. 2010. Functionally distinct hematopoietic stem cells modulate hematopoietic lineage potential during aging by a mechanism of clonal expansion. *Proc. Natl. Acad. Sci. USA.* 107:5465–5470. http://dx.doi.org/10.1073/pnas.1000834107

Bengtsson, T., and M. Lindstrom. 2003. Airborne infectious diseases during infancy and mortality in later life in southern Sweden, 1766-1894. *Int. J. Epidemiol.* 32:286–294. http://dx.doi.org/10.1093/ije/dyg061

Biernacka, A., and N.G. Frangogiannis. 2011. Aging and cardiac fibrosis. *Aging Dis.* 2:158–173.

Borissoff, J.I., I.A. Joosen, M.O. Versteylen, A. Brill, T.A. Fuchs, A.S. Savchenko, M. Gallant, K. Martinod, H. Ten Cate, L. Hofstra, et al. 2013. Elevated levels of circulating DNA and chromatin are independently associated with severe coronary atherosclerosis and a prothrombotic state. *Arterioscler. Thromb. Vasc. Biol.* 33:2032–2040. http://dx.doi.org/10.1161/ATVBAHA.113.301627

Brill, A., T.A. Fuchs, A.S. Savchenko, G.M. Thomas, K. Martinod, S.F. De Meyer, A.A. Bhandari, and D.D. Wagner. 2012. Neutrophil extracellular traps promote deep vein thrombosis in mice. *J. Thromb. Haemost.* 10:136–144. http://dx.doi.org/10.1111/j.1538-7836.2011.04544.x

Brinkmann, V., U. Reichard, C. Goosmann, B. Fauler, Y. Uhlemann, D.S. Weiss, Y. Weinrauch, and A. Zychlinsky. 2004. Neutrophil extracellular traps kill bacteria. *Science.* 303:1532–1535. http://dx.doi.org/10.1126/science.1092385

Cakman, I., J. Rohwer, R.M. Schutz, H. Kirchner, and L. Rink. 1996. Dysregulation between TH1 and TH2 T cell subpopulations in the elderly. *Mech. Ageing Dev.* 87:197–209. http://dx.doi.org/10.1016/0047-6374(96)01708-3

Caudrillier, A., K. Kessenbrock, B.M. Gilliss, J.X. Nguyen, M.B. Marques, M. Monestier, P. Toy, Z. Werb, and M.R. Looney. 2012. Platelets induce neutrophil extracellular traps in transfusion-related acute lung injury. *J. Clin. Invest.* 122:2661–2671. http://dx.doi.org/10.1172/JCI61303

Chang, X., and J. Han. 2006. Expression of peptidylarginine deiminase type 4 (PAD4) in various tumors. *Mol. Carcinog.* 45:183–196. http://dx.doi.org/10.1002/mc.20169

Chrysanthopoulou, A., I. Mitroulis, E. Apostolidou, S. Arelaki, D. Mikroulis, T. Konstantinidis, E. Sivridis, M. Koffa, A. Giatromanolaki, D.T. Boumpas, et al. 2014. Neutrophil extracellular traps promote differentiation and function of fibroblasts. *J. Pathol.* 233:294–307. http://dx.doi.org/10.1002/path.4359

Chua, F., S.E. Dunsmore, P.H. Clingen, S.E. Mutsaers, S.D. Shapiro, A.W. Segal, J. Roes, and G.J. Laurent. 2007. Mice lacking neutrophil elastase are resistant to bleomycin-induced pulmonary fibrosis. *Am. J. Pathol.* 170:65–74. http://dx.doi.org/10.2353/ajpath.2007.060352

Clark, R.A. 1999. Activation of the neutrophil respiratory burst oxidase. *J. Infect. Dis.* 179(s2):S309–S317. http://dx.doi.org/10.1086/513849

Clark, S.R., A.C. Ma, S.A. Tavener, B. McDonald, Z. Goodarzi, M.M. Kelly, K.D. Patel, S. Chakrabarti, E. McAvoy, G.D. Sinclair, et al. 2007. Platelet TLR4 activates neutrophil extracellular traps to ensnare bacteria in septic blood. *Nat. Med.* 13:463–469. http://dx.doi.org/10.1038/nm1565

Cools-Lartigue, J., J. Spicer, B. McDonald, S. Gowing, S. Chow, B. Giannias, F. Bourdeau, P. Kubes, and L. Ferri. 2013. Neutrophil extracellular traps sequester circulating tumor cells and promote metastasis. *J. Clin. Invest.* 123:3446–3458. http://dx.doi.org/10.1172/JCI67484

Dai, D.F., and P.S. Rabinovitch. 2009. Cardiac aging in mice and humans: the role of mitochondrial oxidative stress. *Trends Cardiovasc. Med.* 19:213–220. http://dx.doi.org/10.1016/j.tcm.2009.12.004

Dai, Z., T. Aoki, Y. Fukumoto, and H. Shimokawa. 2012. Coronary perivascular fibrosis is associated with impairment of coronary blood flow in patients with non-ischemic heart failure. *J. Cardiol.* 60:416–421. http://dx.doi.org/10.1016/j.jjcc.2012.06.009

Downloaded from http://rupress.org/jem/article-pdf/214/2/439/1756691/jem_20160530.pdf by guest on 08 February 2026

DeFrances, C.J., K.A. Cullen, and L.J. Kozak. 2007. National Hospital Discharge Survey: 2005 annual summary with detailed diagnosis and procedure data. *Vital Health Stat. 13*. Dec:1–209.

Demers, M., and D.D. Wagner. 2013. Neutrophil extracellular traps: A new link to cancer-associated thrombosis and potential implications for tumor progression. *OncoImmunology.* 2:e22946. http://dx.doi.org/10.4161/onci.22946

Demers, M., D.S. Krause, D. Schatzberg, K. Martinod, J.R. Voorhees, T.A. Fuchs, D.T. Scadden, and D.D. Wagner. 2012. Cancers predispose neutrophils to release extracellular DNA traps that contribute to cancer-associated thrombosis. *Proc. Natl. Acad. Sci. USA.* 109:13076–13081. http://dx.doi.org/10.1073/pnas.1200419109

De Meyer, S.F., G.L. Suidan, T.A. Fuchs, M. Monestier, and D.D. Wagner. 2012. Extracellular chromatin is an important mediator of ischemic stroke in mice. *Arterioscler. Thromb. Vasc. Biol.* 32:1884–1891. http://dx.doi.org/10.1161/ATVBAHA.112.250993

Diaz, J.A., T.A. Fuchs, T.O. Jackson, J.A. Kremer Hovinga, B. Lämmle, P.K. Henke, D.D. Myers Jr., D.D. Wagner, and T.W. Wakefield. Michigan Research Venous Group. 2013. Plasma DNA is elevated in patients with deep vein thrombosis. *J. Vasc. Surg. Venous Lymphat. Disord.* 1:341–348. http://dx.doi.org/10.1016/j.jvsv.2012.12.002

Dwivedi, N., J. Upadhyay, I. Neeli, S. Khan, D. Pattanaik, L. Myers, K.A. Kirou, B. Hellmich, B. Knuckley, P.R. Thompson, et al. 2012. Felty's syndrome autoantibodies bind to deiminated histones and neutrophil extracellular chromatin traps. *Arthritis Rheum.* 64:982–992. http://dx.doi.org/10.1002/art.33432

Etulain, J., K. Martinod, S.L. Wong, S.M. Cifuni, M. Schattner, and D.D. Wagner. 2015. P-selectin promotes neutrophil extracellular trap formation in mice. *Blood.* 126:242–246. http://dx.doi.org/10.1182/blood-2015-01-624023

Finch, C.E., and E.M. Crimmins. 2004. Inflammatory exposure and historical changes in human life-spans. *Science.* 305:1736–1739. http://dx.doi.org/10.1126/science.1092556

Fuchs, T.A., A. Brill, D. Duerschmied, D. Schatzberg, M. Monestier, D.D. Myers Jr., S.K. Wrobleski, T.W. Wakefield, J.H. Hartwig, and D.D. Wagner. 2010. Extracellular DNA traps promote thrombosis. *Proc. Natl. Acad. Sci. USA.* 107:15880–15885. http://dx.doi.org/10.1073/pnas.1005743107

Fuchs, T.A., A. Brill, and D.D. Wagner. 2012. Neutrophil extracellular trap (NET) impact on deep vein thrombosis. *Arterioscler. Thromb. Vasc. Biol.* 32:1777–1783. http://dx.doi.org/10.1161/ATVBAHA.111.242859

Gavillet, M., K. Martinod, R. Renella, C. Harris, N.I. Shapiro, D.D. Wagner, and D.A. Williams. 2015. Flow cytometric assay for direct quantification of neutrophil extracellular traps in blood samples. *Am. J. Hematol.* 90:1155–1158. http://dx.doi.org/10.1002/ajh.24185

Gazoti Debessa, C.R., L.B. Mesiano Maifrino, and R. Rodrigues de Souza. 2001. Age related changes of the collagen network of the human heart. *Mech. Ageing Dev.* 122:1049–1058. http://dx.doi.org/10.1016/S0047-6374(01)00238-X

Hakkim, A., B.G. Furnrohr, K. Amann, B. Laube, U.A. Abed, V. Brinkmann, M. Herrmann, R.E. Voll, and A. Zychlinsky. 2010. Impairment of neutrophil extracellular trap degradation is associated with lupus nephritis. *Proc. Natl. Acad. Sci. USA.* 107:9813–9818. http://dx.doi.org/10.1073/pnas.0909927107

Higashiyama, H., M. Sugai, H. Inoue, K. Mizuyachi, H. Kushida, S. Asano, and M. Kinoshita. 2007. Histopathological study of time course changes in inter-renal aortic banding-induced left ventricular hypertrophy of mice. *Int. J. Exp. Pathol.* 88:31–38. http://dx.doi.org/10.1111/j.1365-2613.2006.00514.x

Hilgendorf, I., L.M. Gerhardt, T.C. Tan, C. Winter, T.A. Holderried, B.G. Chousterman, Y. Iwamoto, R. Liao, A. Zirlik, M. Scherer-Crosbie, et al. 2014. Ly-6Chigh monocytes depend on Nr4a1 to balance both inflammatory and reparative phases in the infarcted myocardium. *Circ. Res.* 114:1611–1622. http://dx.doi.org/10.1161/CIRCRESAHA.114.303204

Junqueira, L.C., G. Bignolas, and R.R. Brentani. 1979. Picrosirius staining plus polarization microscopy, a specific method for collagen detection in tissue sections. *Histochem. J.* 11:447–455. http://dx.doi.org/10.1007/BF01002772

Kessenbrock, K., M. Krumbholz, U. Schonermarck, W. Back, W.L. Gross, Z. Werb, H.J. Grone, V. Brinkmann, and D.E. Jenne. 2009. Netting neutrophils in autoimmune small-vessel vasculitis. *Nat. Med.* 15:623–625. http://dx.doi.org/10.1038/nm.1959

Kolaczkowska, E., and P. Kubes. 2013. Neutrophil recruitment and function in health and inflammation. *Nat. Rev. Immunol.* 13:159–175. http://dx.doi.org/10.1038/nri3399

Kolaczkowska, E., C.N. Jenne, B.G. Surewaard, A. Thanabalasuriar, W.Y. Lee, M.J. Sanz, K. Mowen, G. Opdenakker, and P. Kubes. 2015. Molecular mechanisms of NET formation and degradation revealed by intravital imaging in the liver vasculature. *Nat. Commun.* 6:6673. http://dx.doi.org/10.1038/ncomms7673

Kumamoto, T., Y. Kawai, K. Arakawa, N. Morikawa, J. Kuribara, H. Tada, K. Taniguchi, R. Tatami, I. Miyamori, Y. Kominato, et al. 2006. Association of Gln222Arg polymorphism in the deoxyribonuclease I (DNase I) gene with myocardial infarction in Japanese patients. *Eur. Heart J.* 27:2081–2087. http://dx.doi.org/10.1093/eurheartj/ehl177

Li, P., H. Yao, Z. Zhang, M. Li, Y. Luo, P.R. Thompson, D.S. Gilmour, and Y. Wang. 2008. Regulation of p53 target gene expression by peptidylarginine deiminase 4. *Mol. Cell. Biol.* 28:4745–4758. http://dx.doi.org/10.1128/MCB.01747-07

Loffredo, F.S., A.P. Nikolova, J.R. Pancoast, and R.T. Lee. 2014. Heart failure with preserved ejection fraction: molecular pathways of the aging myocardium. *Circ. Res.* 115:97–107. http://dx.doi.org/10.1161/CIRCRESAHA.115.302929

Lorell, B.H., and B.A. Carabello. 2000. Left ventricular hypertrophy: pathogenesis, detection, and prognosis. *Circulation.* 102:470–479. http://dx.doi.org/10.1161/01.CIR.102.4.470

Martinod, K., and D.D. Wagner. 2014. Thrombosis: tangled up in NETs. *Blood.* 123:2768–2776. http://dx.doi.org/10.1182/blood-2013-10-463646

Martinod, K., M. Demers, T.A. Fuchs, S.L. Wong, A. Brill, M. Gallant, J. Hu, Y. Wang, and D.D. Wagner. 2013. Neutrophil histone modification by peptidylarginine deiminase 4 is critical for deep vein thrombosis in mice. *Proc. Natl. Acad. Sci. USA.* 110:8674–8679. http://dx.doi.org/10.1073/pnas.1301059110

Meyer, A., W. Wang, J. Qu, L. Croft, J.L. Degen, B.S. Coller, and J. Ahamed. 2012. Platelet TGF-β1 contributions to plasma TGF-β1, cardiac fibrosis, and systolic dysfunction in a mouse model of pressure overload. *Blood.* 119:1064–1074. http://dx.doi.org/10.1182/blood-2011-09-377648

Meyer, K.C., N.S. Rosenthal, P. Soergel, and K. Peterson. 1998. Neutrophils and low-grade inflammation in the seemingly normal aging human lung. *Mech. Ageing Dev.* 104:169–181. http://dx.doi.org/10.1016/S0047-6374(98)00065-7

Namba, T., H. Tsutsui, H. Tagawa, M. Takahashi, K. Saito, T. Kozai, M. Usui, K. Imanaka-Yoshida, T. Imaizumi, and A. Takeshita. 1997. Regulation of fibrillar collagen gene expression and protein accumulation in volume-overloaded cardiac hypertrophy. *Circulation.* 95:2448–2454. http://dx.doi.org/10.1161/01.CIR.95.10.2448

National Institute on Aging. 2011. Why Population Aging Matters to Health: A Global Perspective. National Institutes of Health. Available at: https://www.nia.nih.gov/research/publication/global-health-and-aging/overview (accessed November, 2014).

Navaratnam, V., K.M. Fleming, J. West, C.J. Smith, R.G. Jenkins, A. Fogarty, and R.B. Hubbard. 2011. The rising incidence of idiopathic pulmonary fibrosis in the U.K. *Thorax.* 66:462–467. http://dx.doi.org/10.1136/thx.2010.148031

Downloaded from http://rupress.org/jem/article-pdf/214/2/439/1756691/jem_20160530.pdf by guest on 08 February 2026

Ogawa, K., K. Suzuki, M. Okutsu, K. Yamazaki, and S. Shinkai. 2008. The association of elevated reactive oxygen species levels from neutrophils with low-grade inflammation in the elderly. *Immun. Ageing.* 5:13. http://dx.doi.org/10.1186/1742-4933-5-13

Parker, H., M. Dragunow, M.B. Hampton, A.J. Kettle, and C.C. Winterbourn. 2012. Requirements for NADPH oxidase and myeloperoxidase in neutrophil extracellular trap formation differ depending on the stimulus. *J. Leukoc. Biol.* 92:841–849. http://dx.doi.org/10.1189/jlb.1211601

Patel, K.D., G.A. Zimmerman, S.M. Prescott, R.P. McEver, and T.M. McIntyre. 1991. Oxygen radicals induce human endothelial cells to express GMP-140 and bind neutrophils. *J. Cell Biol.* 112:749–759. http://dx.doi.org/10.1083/jcb.112.4.749

Pillai, P.S., R.D. Molony, K. Martinod, H. Dong, I.K. Pang, M.C. Tal, A.G. Solis, P. Bielecki, S. Mohanty, M. Trentalange, et al. 2016. Mx1 reveals innate pathways to antiviral resistance and lethal influenza disease. *Science.* 352:463–466. http://dx.doi.org/10.1126/science.aaf3926

Pugh, K.G., and J.Y. Wei. 2001. Clinical implications of physiological changes in the aging heart. *Drugs Aging.* 18:263–276. http://dx.doi.org/10.2165/00002512-200118040-00004

Quillard, T., H.A. Araujo, G. Franck, E. Shvartz, G. Sukhova, and P. Libby. 2015. TLR2 and neutrophils potentiate endothelial stress, apoptosis and detachment: implications for superficial erosion. *Eur. Heart J.* 36:1394–1404. http://dx.doi.org/10.1093/eurheartj/ehv044

Radic, M., and T.N. Marion. 2013. Neutrophil extracellular chromatin traps connect innate immune response to autoimmunity. *Semin. Immunopathol.* 35:465–480. http://dx.doi.org/10.1007/s00281-013-0376-6

Savchenko, A.S., J.I. Borissoff, K. Martinod, S.F. De Meyer, M. Gallant, L. Erpenbeck, A. Brill, Y. Wang, and D.D. Wagner. 2014a. VWF-mediated leukocyte recruitment with chromatin decondensation by PAD4 increases myocardial ischemia/reperfusion injury in mice. *Blood.* 123:141–148. http://dx.doi.org/10.1182/blood-2013-07-514992

Savchenko, A.S., K. Martinod, M.A. Seidman, S.L. Wong, J.I. Borissoff, G. Piazza, P. Libby, S.Z. Goldhaber, R.N. Mitchell, and D.D. Wagner. 2014b. Neutrophil extracellular traps form predominantly during the organizing stage of human venous thromboembolism development. *J. Thromb. Haemost.* 12:860–870. http://dx.doi.org/10.1111/jth.12571

Schröder, A.K., and L. Rink. 2003. Neutrophil immunity of the elderly. *Mech. Ageing Dev.* 124:419–425. http://dx.doi.org/10.1016/S0047-6374(03)00017-4

Sirker, A., M. Zhang, C. Murdoch, and A.M. Shah. 2007. Involvement of NADPH oxidases in cardiac remodelling and heart failure. *Am. J. Nephrol.* 27:649–660. http://dx.doi.org/10.1159/000109148

Siwik, D.A., P.J. Pagano, and W.S. Colucci. 2001. Oxidative stress regulates collagen synthesis and matrix metalloproteinase activity in cardiac fibroblasts. *Am. J. Physiol. Cell Physiol.* 280:C53–C60.

Sohal, R.S., and R. Weindruch. 1996. Oxidative stress, caloric restriction, and aging. *Science.* 273:59–63. http://dx.doi.org/10.1126/science.273.5271.59

Sun, M., M. Chen, F. Dawood, U. Zurawska, J.Y. Li, T. Parker, Z. Kassiri, L.A. Kirshenbaum, M. Arnold, R. Khokha, and P.P. Liu. 2007. Tumor necrosis factor-alpha mediates cardiac remodeling and ventricular dysfunction after pressure overload state. *Circulation.* 115:1398–1407. http://dx.doi.org/10.1161/CIRCULATIONAHA.106.643585

Sur Chowdhury, C., S. Giaglis, U.A. Walker, A. Buser, S. Hahn, and P. Hasler. 2014. Enhanced neutrophil extracellular trap generation in rheumatoid arthritis: analysis of underlying signal transduction pathways and potential diagnostic utility. *Arthritis Res. Ther.* 16:R122. http://dx.doi.org/10.1186/ar4579

Tabas, I., and C.K. Glass. 2013. Anti-inflammatory therapy in chronic disease: challenges and opportunities. *Science.* 339:166–172. http://dx.doi.org/10.1126/science.1230720

Tarnavski, O., J.R. McMullen, M. Schinke, Q. Nie, S. Kong, and S. Izumo. 2004. Mouse cardiac surgery: comprehensive techniques for the generation of mouse models of human diseases and their application for genomic studies. *Physiol. Genomics.* 16:349–360.

Thévenaz, P., and M. Unser. 2007. User-friendly semiautomated assembly of accurate image mosaics in microscopy. *Microsc. Res. Tech.* 70:135–146. http://dx.doi.org/10.1002/jemt.20393

Thomas, G.M., C. Carbo, B.R. Curtis, K. Martinod, I.B. Mazo, D. Schatzberg, S.M. Cifuni, T.A. Fuchs, U.H. von Andrian, J.H. Hartwig, et al. 2012. Extracellular DNA traps are associated with the pathogenesis of TRALI in humans and mice. *Blood.* 119:6335–6343. http://dx.doi.org/10.1182/blood-2012-01-405183

van Beers, J.J., A.J. Zendman, R. Raijmakers, J. Stammen-Vogelzangs, and G.J. Pruijn. 2013. Peptidylarginine deiminase expression and activity in PAD2 knock-out and PAD4-low mice. *Biochimie.* 95:299–308. http://dx.doi.org/10.1016/j.biochi.2012.09.029

van Durme, Y.M., K.M. Verhamme, T. Stijnen, F.J. van Rooij, G.R. Van Pottelberge, A. Hofman, G.F. Joos, B.H. Stricker, and G.G. Brusselle. 2009. Prevalence, incidence, and lifetime risk for the development of COPD in the elderly: the Rotterdam study. *Chest.* 135:368–377. http://dx.doi.org/10.1378/chest.08-0684

Varagic, J., D. Susic, and E. Frohlich. 2001. Heart, aging, and hypertension. *Curr. Opin. Cardiol.* 16:336–341. http://dx.doi.org/10.1097/00001573-200111000-00004

Wagner, D.D., and P.S. Frenette. 2008. The vessel wall and its interactions. *Blood.* 111:5271–5281. http://dx.doi.org/10.1182/blood-2008-01-078204

Wang, Y., J. Wysocka, J. Sayegh, Y.H. Lee, J.R. Perlin, L. Leonelli, L.S. Sonbuchner, C.H. McDonald, R.G. Cook, Y. Dou, et al. 2004. Human PAD4 regulates histone arginine methylation levels via demethylimination. *Science.* 306:279–283. http://dx.doi.org/10.1126/science.1101400

Wang, Y., M. Li, S. Stadler, S. Correll, P. Li, D. Wang, R. Hayama, L. Leonelli, H. Han, S.A. Grigoryev, et al. 2009. Histone hypercitrullination mediates chromatin decondensation and neutrophil extracellular trap formation. *J. Cell Biol.* 184:205–213. http://dx.doi.org/10.1083/jcb.200806072

Warnatsch, A., M. Ioannou, Q. Wang, and V. Papayannopoulos. 2015. Inflammation. Neutrophil extracellular traps license macrophages for cytokine production in atherosclerosis. *Science.* 349:316–320. http://dx.doi.org/10.1126/science.aaa8064

Wei, J.Y. 1992. Age and the cardiovascular system. *N. Engl. J. Med.* 327:1735–1739. http://dx.doi.org/10.1056/NEJM199212103272408

Weisheit, C., Y. Zhang, A. Faron, O. Kopke, G. Weisheit, A. Steinstrasser, S. Frede, R. Meyer, O. Boehm, A. Hoeft, et al. 2014. $Ly6C^{low}$ and not $Ly6C^{high}$ macrophages accumulate first in the heart in a model of murine pressure-overload. *PLoS One.* 9:e112710. http://dx.doi.org/10.1371/journal.pone.0112710

Woessner, J.F. Jr. 1961. The determination of hydroxyproline in tissue and protein samples containing small proportions of this imino acid. *Arch. Biochem. Biophys.* 93:440–447. http://dx.doi.org/10.1016/0003-9861(61)90291-0

Wong, S.L., M. Demers, K. Martinod, M. Gallant, Y. Wang, A.B. Goldfine, C.R. Kahn, and D.D. Wagner. 2015. Diabetes primes neutrophils to undergo NETosis, which impairs wound healing. *Nat. Med.* 21:815–819. http://dx.doi.org/10.1038/nm.3887

Wynn, T.A., and T.R. Ramalingam. 2012. Mechanisms of fibrosis: therapeutic translation for fibrotic disease. *Nat. Med.* 18:1028–1040. http://dx.doi.org/10.1038/nm.2807

Xu, J., X. Zhang, R. Pelayo, M. Monestier, C.T. Ammollo, F. Semeraro, F.B. Taylor, N.L. Esmon, F. Lupu, and C.T. Esmon. 2009. Extracellular histones are major mediators of death in sepsis. *Nat. Med.* 15:1318–1321. http://dx.doi.org/10.1038/nm.2053

Downloaded from http://rupress.org/jem/article-pdf/214/2/439/1756691/jem_20160530.pdf by guest on 08 February 2026

Yang, B., D.F. Larson, and R. Watson. 1999. Age-related left ventricular function in the mouse: analysis based on in vivo pressure-volume relationships. *Am. J. Physiol.* 277:H1906–H1913.

Zenaro, E., E. Pietronigro, V. Della Bianca, G. Piacentino, L. Marongiu, S. Budui, E. Turano, B. Rossi, S. Angiari, S. Dusi, et al. 2015. Neutrophils promote Alzheimer's disease-like pathology and cognitive decline via LFA-1 integrin. *Nat. Med.* 21:880–886. http://dx.doi.org/10.1038/nm.3913

Zhang, D., G. Chen, D. Manwani, A. Mortha, C. Xu, J.J. Faith, R.D. Burk, Y. Kunisaki, J.E. Jang, C. Scheiermann, et al. 2015. Neutrophil ageing is regulated by the microbiome. *Nature.* 525:528–532. http://dx.doi.org/10.1038/nature15367

Downloaded from http://rupress.org/jem/article-pdf/214/2/439/1756691/jem_20160530.pdf by guest on 08 February 2026